

# Bootstrap Prediction Bands for Functional Time Series

Efstathios Paparoditis

Department of Mathematics and Statistics  
University of Cyprus

Han Lin Shang

Department of Actuarial Studies and Business Analytics  
Macquarie University  
Research School of Finance, Actuarial Studies and Statistics  
Australian National University

## Abstract

A bootstrap procedure for constructing pointwise or simultaneous prediction intervals for a stationary functional time series is proposed. The procedure exploits a general vector autoregressive representation of the time-reversed series of Fourier coefficients appearing in the Karhunen-Loève representation of the functional process. It generates backwards-in-time, functional replicates that adequately mimic the dependence structure of the underlying process and have the same conditionally fixed curves at the end of each functional pseudo-time series. The bootstrap prediction error distribution is then calculated as the difference between the model-free, bootstrap-generated future functional observations and the functional forecasts obtained from the model used for prediction. This allows the estimated prediction error distribution to account for not only the innovation and estimation errors associated with prediction but also the possible errors from model misspecification. We show the asymptotic validity of the bootstrap in estimating the prediction error distribution of interest. Furthermore, the bootstrap procedure allows for the construction of prediction bands that achieve (asymptotically) the desired coverage. These prediction bands are based on a consistent estimation of the distribution of the studentized prediction error process. Through a simulation study and the analysis of two data sets, we demonstrate the capabilities and the good finite-sample performance of the proposed method.

**Keywords:** Fourier transform; Functional prediction; Prediction error; Principal components; Karhunen-Loève expansion.

# 1 Introduction

Functional time series consist of random functions observed at regular time intervals. Functional time series can be classified into two main categories depending on whether or not the continuum is also a time variable. First, functional time series can arise from measurements obtained by separating an almost continuous time record into consecutive intervals (e.g., days, weeks, or years; see, e.g., [Hörmann and Kokoszka, 2012](#)). We refer to such data structures as sliced functional time series, examples of which include daily price curves of a financial stock ([Kokoszka et al., 2017](#)) and intraday particulate matter ([Shang, 2017](#)). In contrast, when the continuum is not a time variable, functional time series can also arise when observations over a period are considered as finite dimensional realizations of an underlying continuous function (e.g., yearly age-specific mortality rates; see, e.g., [Chiou and Müller, 2009](#); [Hyndman and Shang, 2009](#)).

In either case, the underlying stochastic process is denoted by  $\mathbf{X} = \{\mathcal{X}_t, t \in \mathbb{Z}\}$ ,  $\mathbb{Z} = \{t : t \in 0, \pm 1, \dots\}$ , where each  $\mathcal{X}_t$  is a random element in a separable Hilbert space  $\mathcal{H}$ , with values  $\mathcal{X}_t(\tau)$  and  $\tau$  taking values within a compact interval  $\mathcal{I} \subset \mathbb{R}$ . Without loss of generality we assume in this paper that  $\mathcal{I} = [0, 1]$ . Central statistical issues include modeling of the temporal dependence of the functional random variables  $\{\mathcal{X}_t, t \in \mathbb{Z}\}$ , making inferences about parameters of interest, and predicting future values of the process when an observed stretch  $\mathcal{X}_1, \mathcal{X}_2, \dots, \mathcal{X}_n$  is given. Not only is it vital to obtain consistent estimators, but to also estimate the uncertainty associated with such estimators, the construction of confidence or prediction intervals, and the implementation of hypothesis tests (e.g., [Horváth et al., 2014](#)). When such inference problems arise in functional time series, a resampling methodology, especially bootstrapping, is an important alternative to standard asymptotic considerations. For independent and identically distributed (i.i.d.) functional data, we refer to [Cuevas et al. \(2006\)](#); [McMurry and Politis \(2011\)](#); [Goldsmith et al. \(2013\)](#); [Shang \(2015\)](#); [Paparoditis and Sapatinas \(2016\)](#), in which appropriate sampling from the observed sample is used to mimic sampling from the population. However, for functional time series, the existing temporal dependence between the random elements  $\mathcal{X}_t$  significantly complicates matters, and the bootstrap must be appropriately adapted to be successful.

The development of bootstrap procedures for functional time series has received increasing attention in recent decades. In an early paper, [Politis and Romano \(1994a\)](#) obtained weak convergence results for approximate sums of weakly dependent, Hilbert space-valued random variables in a triangular array setting, validating the bootstrap central limit theorem for the stationary bootstrap. [Dehling et al. \(2015\)](#) also obtained weak convergence results for Hilbert space-valued random variables, which are assumed to be weakly dependent in the sense of near-epoch dependence, showing the consistency of a non-overlapping block bootstrap procedure. [Raña et al. \(2015\)](#) extended the stationary bootstrap procedure of [Politis and Romano \(1994b\)](#) to a functional time series. [Ferraty and Vieu \(2011\)](#) applied a residual-based bootstrap procedure to construct confidence intervals for the regression function in the nonparametric functional regression setting. [Franke and Nyarige \(2019\)](#) proposed a residual-based bootstrap procedure for functional autoregressions (see also [Pan and Politis, 2016](#)). [Pilavakis et al. \(2019\)](#) established some theoretical results for the moving block and the tapered block bootstrap, [Shang \(2018\)](#) applied a maximum entropy bootstrap procedure, and [Paparoditis \(2018\)](#) proposed a sieve bootstrap procedure for functional time series.

In this paper, we build on the developments mentioned above and focus on the problem of constructing prediction intervals or bands for a functional time series. To elaborate, suppose that for every  $t \in \mathbb{Z}$ , the zero mean random elements  $\mathcal{X}_t$  is generated as

$$\mathcal{X}_t = f(\mathcal{X}_{t-1}, \mathcal{X}_{t-2}, \dots) + \varepsilon_t,$$

where  $f : \mathcal{H}^\infty \rightarrow \mathcal{H}$  is some appropriate operator and  $\{\varepsilon_t\}$  is a zero mean i.i.d. innovation process in  $\mathcal{H}$  with  $E\|\varepsilon_t\|^2 < \infty$ . For simplicity, we write  $\varepsilon_t \sim i.i.d.(0, C_\varepsilon)$ , where  $C_\varepsilon = E(\varepsilon_t \otimes \varepsilon_t)$  is the covariance operator of  $\varepsilon_t$  and  $\otimes$  denotes the tensor operator, defined by  $(x \otimes y)(\cdot) = \langle x, \cdot \rangle y$  for  $x, y \in \mathcal{H}$ . Suppose that the model

$$\mathcal{X}_t = g(\mathcal{X}_{t-1}, \mathcal{X}_{t-2}, \dots, \mathcal{X}_{t-k}) + v_t \tag{1}$$

is used for prediction, where  $k < n$  is a fixed integer,  $g : \mathcal{H}^k \rightarrow \mathcal{H}$  is an unknown operator, and  $v_t \sim i.i.d.(0, C_v)$ . The simple case, where  $g$  is known up to a finite dimensional vector of

parameters also is included in the above setup. Given the functional time series  $\mathcal{X}_1, \mathcal{X}_2, \dots, \mathcal{X}_n$ , one-step-ahead prediction of  $\mathcal{X}_{n+1}$  using model (1) is obtained as

$$\hat{\mathcal{X}}_{n+1} = \hat{g}(\mathcal{X}_n, \mathcal{X}_{n-1}, \dots, \mathcal{X}_{n-k+1}), \quad (2)$$

where  $\hat{g}$  denotes an estimator of the operator  $g$ . Although our approach can be extended to the problem of  $h$ -step-ahead prediction for  $h > 1$ , in the following and for simplicity, we consider the case of one-step-ahead prediction only ( $h = 1$ ). The prediction error  $\mathcal{E}_{n+1} = \mathcal{X}_{n+1} - \hat{\mathcal{X}}_{n+1}$  can then be decomposed as

$$\begin{aligned} \mathcal{E}_{n+1} &:= \mathcal{X}_{n+1} - \hat{\mathcal{X}}_{n+1} \\ &= \varepsilon_{n+1} \\ &\quad + \left[ f(\mathcal{X}_n, \mathcal{X}_{n-1}, \dots) - g(\mathcal{X}_n, \mathcal{X}_{n-1}, \dots, \mathcal{X}_{n-k+1}) \right] \\ &\quad + \left[ g(\mathcal{X}_n, \mathcal{X}_{n-1}, \dots, \mathcal{X}_{n-k+1}) - \hat{g}(\mathcal{X}_n, \mathcal{X}_{n-1}, \dots, \mathcal{X}_{n-k+1}) \right] \\ &= \mathcal{E}_{I,n+1} + \mathcal{E}_{M,n+1} + \mathcal{E}_{E,n+1}, \end{aligned}$$

with an obvious notation for  $\mathcal{E}_{I,n+1}$ ,  $\mathcal{E}_{M,n+1}$  and  $\mathcal{E}_{E,n+1}$ . Notice that  $\mathcal{E}_{I,n+1}$  is the error attributable to the i.i.d. innovation,  $\mathcal{E}_{M,n+1}$  is the model specification error, and  $\mathcal{E}_{E,n+1}$  is the error attributable to estimation of the unknown operator  $g$  used for prediction. Observe that if  $\hat{g}$  is a consistent estimator of  $g$ , for instance, if  $\|\hat{g} - g\|_{\mathcal{L}} \xrightarrow{P} 0$ , with  $\|\cdot\|_{\mathcal{L}}$  being the operator norm, the estimation error  $\mathcal{E}_{E,n+1}$  is asymptotically negligible. On the contrary, the misspecification error  $\mathcal{E}_{M,n+1}$  may not vanish asymptotically if the model used for prediction is different to the one generating the data, that is if  $f \neq g$ .

To illustrate this, consider the following example. Suppose that  $\mathcal{X}_t$  is generated according to the FAR(2) model  $\mathcal{X}_t = \Phi_1(\mathcal{X}_{t-1}) + \Phi_2(\mathcal{X}_{t-2}) + \varepsilon_t$ ,  $\Phi_2 \neq 0$ , while a FAR(1) model  $\mathcal{X}_t = R(\mathcal{X}_{t-1}) + v_t$  is used for prediction, where  $\Phi_1$ ,  $\Phi_2$ , and  $R$  are appropriate operators. In general,  $R \neq \Phi_1$ . With  $\hat{R}$  denoting an estimator of  $R$ , the prediction error  $\mathcal{E}_{n+1}$  can be decomposed as

$$\mathcal{X}_{n+1} - \hat{\mathcal{X}}_{n+1} = \varepsilon_{n+1} + (\Phi_1(\mathcal{X}_n) - R(\mathcal{X}_n) + \Phi_2(\mathcal{X}_{n-1})) + (R(\mathcal{X}_n) - \hat{R}(\mathcal{X}_n)).$$

Notice that the model specification error  $(\Phi_1(\mathcal{X}_n) - R(\mathcal{X}_n) + \Phi_2(\mathcal{X}_{n-1}))$  causes a shift in the conditional distribution of  $\mathcal{E}_{n+1}$  given  $\mathcal{X}_n$  due to the term  $\Phi_1(\mathcal{X}_n) - R(\mathcal{X}_n)$  as well as an increase in variability due to the term  $\Phi_2(\mathcal{X}_{n-1})$ .

An appropriate procedure to construct prediction intervals should consider *all three* aforementioned sources affecting the prediction error and consistently estimate the conditional distribution function

$$P[\mathcal{E}_{n+1}(\tau) \leq \cdot | \mathcal{X}_n, \mathcal{X}_{n-1}, \dots, \mathcal{X}_{n-k+1}], \quad \text{for any } \tau \in [0, 1]. \quad (3)$$

However, and to the best of our knowledge, this issue has not been appropriately explored in the literature. In particular, even in the most studied univariate, real-valued case, it is a common approach to estimate the prediction error distribution by ignoring the model specification error, that is, assuming that the model used for prediction is identical to the one generating the observed time series. Consequently, bootstrap approaches applied in this context use the same model for prediction and to generate the bootstrap pseudo-time series; that is, they ignore the model misspecification error (see [Pan and Politis, 2016](#), and the references therein and Section 3 for details).

In this paper, we develop a bootstrap procedure to construct prediction intervals for functional time series that appropriately considers *all three* sources of errors affecting the conditional distribution of  $\mathcal{E}_{n+1}$ . The proposed bootstrap approach generates, in a model-free way, pseudo-replicates  $\mathcal{X}_1^*, \mathcal{X}_2^*, \dots, \mathcal{X}_n^*$ , and  $\mathcal{X}_{n+1}^*$  of the functional time series at hand that mimic the dependence structure of the underlying functional process. Moreover, the approach ensures that the generated functional pseudo-time series has the same  $k$  functions at the end as the functional times series observed; that is,  $\mathcal{X}_t^* = \mathcal{X}_t$  holds for  $t = n - k + 1, n - k + 2, \dots, n$ . This is important because, as Equation (3) shows, it is the conditional distribution of  $\mathcal{E}_{n+1}$  given  $\mathcal{X}_n, \mathcal{X}_{n-1}, \dots, \mathcal{X}_{n-k+1}$  in which we are interested. These requirements are fulfilled by generating the functional pseudo-elements  $\mathcal{X}_1^*, \mathcal{X}_2^*, \dots, \mathcal{X}_n^*$  using a backward-in-time vector autoregressive representation of the time-reversed process of scores appearing in the Karhunen-Loève representation (see Section 2 for details). Given the model-free, bootstrap-generated functional pseudo-time series  $\mathcal{X}_1^*, \mathcal{X}_2^*, \dots, \mathcal{X}_n^*$  and  $\mathcal{X}_{n+1}^*$ , the same model used to obtain

the predictor  $\hat{\mathcal{X}}_{n+1} = \hat{g}(\mathcal{X}_n, \dots, \mathcal{X}_{n-k+1})$ , see (2), is then applied, and the pseudo-predictor  $\hat{\mathcal{X}}_{n+1}^* = \hat{g}^*(\mathcal{X}_n^*, \dots, \mathcal{X}_{n-k+1}^*)$  is obtained. Here,  $\hat{g}^*$  denotes the same estimator as  $\hat{g}$  but based on the generated bootstrap functional pseudo-time series  $\mathcal{X}_1^*, \mathcal{X}_2^*, \dots, \mathcal{X}_n^*$ . The conditional distribution of the prediction error  $\mathcal{X}_{n+1} - \hat{\mathcal{X}}_{n+1}$  is then estimated using the conditional distribution of the bootstrap prediction error  $\mathcal{X}_{n+1}^* - \hat{\mathcal{X}}_{n+1}^*$ . We show that the described procedure leads to consistent estimates of the conditional distribution of interest. We also prove consistency of the bootstrap in estimating the conditional distribution of the studentized prediction error process in  $\mathcal{H}$ . The latter consistency theoretically justifies the use of the proposed bootstrap method in the construction of simultaneous prediction bands that appropriately account for the local variability of the prediction error. Further, we demonstrate by means of simulations and two empirical data applications the good finite sample performance of this bootstrap procedure.

The paper is organized as follows. In Section 2, we state the notation used in this paper and introduce the notion of backward vector autoregressive representations of the time-reversed vector process of scores appearing in the Karhunen-Loève representation. In Section 3, we present the proposed bootstrap procedure and show its asymptotic validity for the construction of pointwise prediction intervals and simultaneous prediction bands. Section 5 investigates the finite sample performance of the proposed bootstrap procedure using simulations, while in Section 6, applications of the new methodology to two real-life data sets are considered. Conclusions are provided in Section 7. Proofs and auxiliary lemmas are given in Appendix A.

## 2 Preliminaries

### 2.1 Setup and Examples of Predictors

Consider a time series  $\mathcal{X}_1, \mathcal{X}_2, \dots, \mathcal{X}_n$  stemming from a stationary,  $L^2$ - $\mathcal{M}$ -approximable stochastic process  $\mathbf{X} = \{\mathcal{X}_t, t \in \mathbb{Z}\}$  with mean  $E(\mathcal{X}_t) = 0$  and autocovariance operator  $C_h = E(\mathcal{X}_t \otimes \mathcal{X}_{t+h})$ ,  $h \in \mathbb{Z}$  (recall that  $C_h$  is a Hilbert-Schmidt (HS) operator). The  $L^2$ -m-approximability property implies that  $\sum_{h \in \mathbb{Z}} \|C_h\|_{\text{HS}} < \infty$  and therefore, that the functional process  $\mathbf{X}$  possesses

a continuous and self-adjoint spectral density operator  $\mathcal{F}_\omega$ , given by

$$\mathcal{F}_\omega = (2\pi)^{-1} \sum_{h \in \mathbb{Z}} C_h e^{-ih\omega}, \omega \in \mathbb{R},$$

which is trace class (Hörmann et al., 2015) (also see Panaretos and Tavakoli (2013) for a different set of weak dependence conditions on the functional process  $\mathbf{X}$ ). We assume that the eigenvalues  $\nu_1(\omega), \nu_2(\omega), \dots, \nu_m(\omega)$  of the spectral density operator  $\mathcal{F}_\omega$  are strictly positive for every  $\omega \in [0, \pi]$ .

Suppose that the one-step-ahead predictor of  $\mathcal{X}_{n+1}$  is given by

$$\hat{\mathcal{X}}_{n+1} = \hat{g}(\mathcal{X}_n, \dots, \mathcal{X}_{n-k+1}), \quad (4)$$

where  $k \in \mathbb{N}$ ,  $k < n$  is fixed and determined by the model selected to perform the prediction (see (1)), while  $\hat{g}$  denotes an estimator of the unknown operator  $g$ . Based on  $\hat{\mathcal{X}}_{n+1}$ , our aim is to construct a prediction interval for  $\mathcal{X}_{n+1}$ . To achieve this, an estimator of the distribution of the prediction error  $\mathcal{E}_{n+1} = \mathcal{X}_{n+1} - \hat{\mathcal{X}}_{n+1}$  is needed. More precisely, we are interested in estimating the conditional distribution

$$\mathcal{E}_{n+1}(\tau) | \mathcal{X}_n, \mathcal{X}_{n-1}, \dots, \mathcal{X}_{n-k+1}, \text{ for any } \tau \in [0, 1]. \quad (5)$$

Because we do not want to restrict our considerations to a specific predictor  $\hat{g}$ , many of the predictors applied in the functional time series literature can fit in the above setup. Here, we elaborate on some common examples:

- 1) Suppose that  $g(\mathcal{X}_n, \dots, \mathcal{X}_{n-k+1}) = \sum_{j=1}^k \Phi_j(\mathcal{X}_{n+1-j})$  with the  $\Phi_j$ 's being bounded and linear operators  $\Phi_j : \mathcal{H} \rightarrow \mathcal{H}$ . This is a case where a functional autoregressive model of order  $k$  (FAR( $k$ )) is used to predict  $\mathcal{X}_{n+1}$ , see (Kokoszka and Reimherr, 2013b) in which the issue of the selection of the order  $k$  is also discussed. Given some estimators  $\hat{\Phi}_j$  of  $\Phi_j$ , the corresponding predictor is given by  $\hat{g}(\mathcal{X}_n, \dots, \mathcal{X}_{n-k+1}) = \sum_{j=1}^k \hat{\Phi}_j(\mathcal{X}_{n+1-j})$ . A special case is the popular FAR(1) model in which it is assumed that  $\mathcal{X}_t$  is generated as  $\mathcal{X}_t = \Phi(\mathcal{X}_{t-1}) + \varepsilon_t$  with  $\|\Phi\|_{\mathcal{L}} < 1$  and  $\varepsilon_t$  an i.i.d. sequence in  $\mathcal{H}$  (Bosq, 2000; Bosq and

Blanke, 2007).

- 2) Suppose that  $g(\mathcal{X}_n, \dots, \mathcal{X}_{n-k+1}) = \sum_{j=1}^d \mathbf{1}_j^\top \sum_{l=1}^k D_l \xi_{n+1-l} v_j$ , where  $\mathbf{1}_j$  is the  $d$ -dimensional vector with the  $j^{\text{th}}$  component equal to 1 and 0 elsewhere,  $\xi_t$  is the  $d$ -dimensional vector  $\xi_t = (\langle \mathcal{X}_t, v_j \rangle, j = 1, 2, \dots, d)^\top$ ,  $v_j$  are the orthonormal eigenfunctions corresponding to the  $d$  largest eigenvalues of the lag-0 covariance operator  $C_0 = E(\mathcal{X}_0 \otimes \mathcal{X}_0)$ , and  $(D_1, D_2, \dots, D_k)$  are the matrices obtained by the orthogonal projection of  $\xi_t$  on the space spanned by  $(\xi_{t-1}, \xi_{t-2}, \dots, \xi_{t-k})$ . A predictor  $\hat{\mathcal{X}}_{n+1}$  can then be obtained as

$$\hat{g}(\mathcal{X}_n, \dots, \mathcal{X}_{n-k+1}) = \sum_{j=1}^d \mathbf{1}_j^\top \check{\xi}_{n+1} \hat{v}_j,$$

where  $\check{\xi}_{n+1} = \sum_{l=1}^k \hat{D}_l \hat{\xi}_{n+1-l}$ ,  $\hat{\xi}_1, \dots, \hat{\xi}_n$  are the estimated  $d$ -dimensional score vectors  $\hat{\xi}_t = (\langle \mathcal{X}_t, \hat{v}_j \rangle, j = 1, 2, \dots, d)^\top$ ,  $\hat{v}_j$  are the estimated orthonormal eigenfunctions corresponding to the  $d$  largest estimated eigenvalues of  $\hat{C}_0 = n^{-1} \sum_{t=1}^n (\mathcal{X}_t - \bar{\mathcal{X}}_n) \otimes (\mathcal{X}_t - \bar{\mathcal{X}}_n)$  and  $(\hat{D}_l, l = 1, 2, \dots, k)$  are the estimated  $d \times d$  matrices obtained by least squares fitting of a  $k^{\text{th}}$  order vector autoregression to the time series  $\hat{\xi}_t, t = 1, 2, \dots, n$ ; (Aue et al., 2015).

- 3) Similar to 2), the predictor  $\hat{\mathcal{X}}_{n+1}$  can be obtained as  $\hat{g}(\mathcal{X}_n, \dots, \mathcal{X}_{n-k+1}) = \sum_{j=1}^d \mathbf{1}_j^\top \check{\epsilon}_{n+1,j} \hat{v}_j$ , where  $\check{\epsilon}_{n+1,j}$  is obtained via a univariate time series forecasting method, based on the estimated residuals  $(\hat{\epsilon}_{1,j}, \dots, \hat{\epsilon}_{n,j})$  for each  $j = 1, \dots, d$ , (Hyndman and Shang, 2009).
- 4) Let  $k = 1$  and  $g(\mathcal{X}_n) = E(\mathcal{X}_{n+1} | \mathcal{X}_n)$  be the conditional mean function of  $\mathcal{X}_{n+1}$  given  $\mathcal{X}_n$ . The corresponding predictor  $\hat{\mathcal{X}}_{n+1}$  in this case is obtained by using a nonparametric estimator of  $g$ , for instance, a functional version of the Nadaraya-Watson estimator given by

$$\hat{g}_h(\mathcal{X}) = \sum_{i=1}^{n-1} \frac{K[d(\mathcal{X}_i, \mathcal{X})/h] \mathcal{X}_{i+1}}{\sum_{j=1}^{n-1} K[d(\mathcal{X}_j, \mathcal{X})/h]},$$

where  $K(\cdot)$  is a kernel function,  $h > 0$  is a smoothing bandwidth, and  $d(\cdot, \cdot)$  is a distance function on  $\mathcal{H}$ . The corresponding predictor of  $\mathcal{X}_{n+1}$  is then given by  $\hat{\mathcal{X}}_{n+1} = \hat{g}_h(\mathcal{X}_n)$ ; (see, e.g., Antoniadis et al., 2006).



## 2.2 The Time-Reversed Process of Scores

To introduce the proposed bootstrap procedure, it is important to first discuss some properties of the time-reversed process of scores associated with the functional process  $\mathbf{X}$ .

For  $m \in \mathbb{N}$ , consider the  $m$ -dimensional vector process of scores  $\boldsymbol{\xi} = \{\boldsymbol{\xi}_t, t \in \mathbb{Z}\}$ , where  $\boldsymbol{\xi}_t = (\langle \mathcal{X}_t, v_j \rangle, j = 1, 2, \dots, m)^\top$ . Denote by  $\tilde{\boldsymbol{\xi}} = \{\tilde{\boldsymbol{\xi}}_t, t \in \mathbb{Z}\}$  the time-reversed version of  $\boldsymbol{\xi}$ , that is,  $\tilde{\boldsymbol{\xi}}_t = \boldsymbol{\xi}_{-t}$  for any  $t \in \mathbb{Z}$ . We call  $\boldsymbol{\xi}$  and  $\tilde{\boldsymbol{\xi}}$  the forward and backward score processes, respectively. The autocovariance structure of both processes is closely related because for any  $h \in \mathbb{Z}$  we have

$$\begin{aligned} \Gamma_{\tilde{\boldsymbol{\xi}}}(h) &:= E \left[ \tilde{\boldsymbol{\xi}}_0(m) \tilde{\boldsymbol{\xi}}_h^\top(m) \right] \\ &= E \left[ \boldsymbol{\xi}_0(m) \boldsymbol{\xi}_{-h}^\top(m) \right] \\ &=: \Gamma_{\boldsymbol{\xi}}(-h). \end{aligned} \tag{6}$$

Thus, properties of the forward score process  $\boldsymbol{\xi}$ , which arise from its second-order structure, carry over to the backward process  $\tilde{\boldsymbol{\xi}}$ . In particular, the (Hilbert-Schmidt) norm summability of the autocovariance operators  $C_h$  as well as the assumption that the eigenvalues  $\nu_1(\omega), \nu_2(\omega), \dots, \nu_m(\omega)$  of the spectral density operator  $\mathcal{F}_\omega$  are bounded away from zero for all  $\omega \in [0, \pi]$ , imply that, like the  $m \times m$  spectral density matrix  $f_{\boldsymbol{\xi}}(\omega) = (2\pi)^{-1} \sum_{h \in \mathbb{Z}} \Gamma_{\boldsymbol{\xi}}(h) e^{-ih\omega}$  of the forward process  $\boldsymbol{\xi}$ , the  $m \times m$  spectral density matrix  $f_{\tilde{\boldsymbol{\xi}}}(\omega) = (2\pi)^{-1} \sum_{h \in \mathbb{Z}} \Gamma_{\tilde{\boldsymbol{\xi}}}(h) e^{-ih\omega}$  of the backward process  $\tilde{\boldsymbol{\xi}}$  is continuous, bounded from above and bounded away from zero from below. These properties of  $f_{\tilde{\boldsymbol{\xi}}}$  follow immediately from the corresponding properties of  $f_{\boldsymbol{\xi}}$  (see Lemma 2.1 of [Paparoditis, 2018](#)) and by taking into account that (6) implies that  $f_{\tilde{\boldsymbol{\xi}}}(\omega) = f_{\boldsymbol{\xi}}^\top(\omega)$  for all  $\omega \in [0, \pi]$ . Therefore, it follows from Lemma 3.5 of [Cheng and Pourahmadi \(1993, p. 116\)](#), that both processes—the process  $\boldsymbol{\xi}$  and the time-reversed process  $\tilde{\boldsymbol{\xi}}$ —obey a so-called vector autoregressive representation. That is, infinite sequences of  $m \times m$  matrices  $\{A_j, j \in \mathbb{N}\}$  and  $\{B_j, j \in \mathbb{N}\}$  as well as full rank  $m$ -dimensional, white noise processes  $\{\mathbf{e}_t, t \in \mathbb{Z}\}$  and  $\{\mathbf{v}_t, t \in \mathbb{Z}\}$  exist such that the random vectors  $\boldsymbol{\xi}_t$  and  $\tilde{\boldsymbol{\xi}}_t$  have, respectively, the following autoregressive representations:

$$\boldsymbol{\xi}_t = \sum_{j=1}^{\infty} A_j \boldsymbol{\xi}_{t-j} + \mathbf{e}_t \tag{7}$$

and

$$\tilde{\xi}_t = \sum_{j=1}^{\infty} B_j \tilde{\xi}_{t-j} + v_t. \quad (8)$$

We refer to (7) and (8) as the forward and backward vector autoregressive representations of  $\xi_t$  and to  $\{e_t\}$  and to  $\{v_t\}$  as the forward and the backward noise processes. We stress here the fact that representations (7) and (8) should not be confused with that of a *linear* vector autoregressive process. This is because the noise processes  $\{e_t\}$  and  $\{v_t\}$  appearing in representations (7) and (8), respectively, are only uncorrelated and not necessarily i.i.d. sequences of random vectors. The autoregressive matrices  $\{A_j\}$  and  $\{B_j\}$  appearing in the above representations also satisfy the summability conditions  $\sum_{j=1}^{\infty} \|A_j\|_F < \infty$  and  $\sum_{j=1}^{\infty} \|B_j\|_F < \infty$ , where  $\|\cdot\|_F$  denotes the Frobenius norm, while the corresponding power series

$$A(z) = I - \sum_{j=1}^{\infty} A_j z^j \quad \text{and} \quad B(z) = I - \sum_{j=1}^{\infty} B_j z^j$$

do not vanish for  $|z| \leq 1$ ; that is,  $A^{-1}(z)$  and  $B^{-1}(z)$  exist for all  $|z| \leq 1$  (see [Cheng and Pourahmadi, 1993](#); [Meyer and Kreiss, 2015](#), for more details on such vector autoregressive representations of weakly stationary processes). Using reversion in time and, specifically, the property that  $\tilde{\xi}_t = \xi_{-t}$ , Equation (8) leads to the expression

$$\xi_t = \sum_{j=1}^{\infty} B_j \xi_{t+j} + v_t, \quad (9)$$

which also can be written as  $B(L^{-1})\xi_t = v_t$ , with the shift operator  $L$  defined by  $L^k \xi_t = \xi_{t-k}$  for any  $k \in \mathbb{Z}$ . Expression (9) implies that the two white noise innovation processes  $\{e_t, t \in \mathbb{Z}\}$  and  $\{v_t, t \in \mathbb{Z}\}$  are related by

$$\begin{aligned} v_t &= B(L^{-1})\xi_t \\ &= B(L^{-1})A^{-1}(L)e_t, \quad t \in \mathbb{Z}. \end{aligned} \quad (10)$$

Notice that (10) generalizes to the vector autoregressive case an analogue expression obtained for the univariate autoregressive case by [Findley \(1986\)](#) and [Breidt et al. \(1995\)](#). Further, and as

relation (10) shows, even if  $\xi_t$  in (7) is a linear process, that is even if  $\{e_t\}$  is an i.i.d. innovation process in  $\mathbb{R}^m$ , the white noise innovation process  $\{v_t\}$  appearing in the time-reversed version (9) is, in general, not an i.i.d. process.

### 3 Bootstrap Prediction Intervals

#### 3.1 Bootstrap Procedure

The basic idea of the proposed bootstrap procedure is to generate a functional time series of pseudo-random elements  $\mathcal{X}_1^*, \mathcal{X}_2^*, \dots, \mathcal{X}_n^*$ , and  $\mathcal{X}_{n+1}^*$ , which appropriately imitate the dependence structure of the functional time series at hand, while satisfying the condition

$$\mathcal{X}_{n-k+1}^* = \mathcal{X}_{n-k+1}, \quad \mathcal{X}_{n-k+2}^* = \mathcal{X}_{n-k+2}, \dots, \mathcal{X}_n^* = \mathcal{X}_n. \quad (11)$$

The above condition is important because, as we have seen, the conditional distribution of  $\mathcal{E}_{n+1}(\cdot)$  given  $\mathcal{X}_n, \mathcal{X}_{n-1}, \dots, \mathcal{X}_{n-k+1}$  is the one in which we are interested. Motivated by the functional sieve bootstrap proposed by Paparoditis (2018), to achieve this, we use the Karhunen-Loève representation of the random element  $\mathcal{X}_t$  and decompose it in two parts:

$$\begin{aligned} \mathcal{X}_t &= \sum_{j=1}^{\infty} \tilde{\xi}_{j,t} v_j \\ &= \underbrace{\sum_{j=1}^m \tilde{\xi}_{j,t} v_j}_{\mathcal{X}_{t,m}} + \underbrace{\sum_{j=m+1}^{\infty} \tilde{\xi}_{j,t} v_j}_{U_{t,m}}. \end{aligned} \quad (12)$$

Recall that  $\tilde{\xi}_{j,t} = \langle \mathcal{X}_t, v_j \rangle$ , where  $v_j, j = 1, 2, \dots$ , are the orthonormal eigenvectors corresponding to the eigenvalues  $\lambda_1 > \lambda_2 > \dots$ , in descending order, of the lag-0 autocovariance operator  $C_0$ . In decomposition (12), the element  $\mathcal{X}_{t,m}$  is considered as the main driving part of  $\mathcal{X}_t$ , while the “remainder”  $U_{t,m}$  is treated as a white noise component. Now, to generate the functional pseudo-time series  $\mathcal{X}_1^*, \mathcal{X}_2^*, \dots, \mathcal{X}_n^*$ , we first bootstrap the  $m$ -dimensional time series of scores by using the backward vector autoregressive representation (9). Using the backward representation allows for the generation of a pseudo-time series of scores  $\xi_1^*, \xi_2^*, \dots, \xi_n^*$ , which satisfies the

condition  $\xi_t^* = \xi_t$  for  $t = n - k + 1, n - k + 2, \dots, n$ . This is important to ensure that the bootstrap-generated time series  $\mathcal{X}_1^*, \mathcal{X}_2^*, \dots, \mathcal{X}_n^*$  fulfills the requirement (11). The backwards-in-time-generated pseudo-time series of scores  $\xi_1^*, \xi_2^*, \dots, \xi_n^*$  can then be transformed to pseudo-replicates of the main driving part  $\mathcal{X}_{t,m}$  by using the equation  $\mathcal{X}_{t,m}^* = \sum_{j=1}^m \xi_{j,t}^* v_j$ . Notice that by constructing  $\xi_t^* = \xi_t$  when  $t = n, n - 1, \dots, n - k + 1$ , we have that  $\mathcal{X}_{t,m}^* = \mathcal{X}_{t,m}$  and, consequently, we can set  $\mathcal{X}_t^* = \mathcal{X}_t$  for the same set of time indices. Adding to the generated  $\mathcal{X}_{t,m}^*$  for the remaining indices  $t = n - k, n - k - 1, \dots, 1$ , an appropriately resampled functional noise  $U_{t,m}^*$ , leads to functional pseudo replicates  $\mathcal{X}_1^*, \mathcal{X}_2^*, \dots, \mathcal{X}_{n-k}^*$ . As a result, a functional pseudo-time series  $\mathcal{X}_1^*, \mathcal{X}_2^*, \dots, \mathcal{X}_n^*$  can be obtained that imitates the dependence structure of  $\mathcal{X}_1, \mathcal{X}_2, \dots, \mathcal{X}_n$  while satisfying (11). Clearly, implementation of the above idea requires estimation of the scores  $\xi_{j,t} = \langle \mathcal{X}_t, v_j \rangle$  and of the eigenvectors  $v_j$  because these quantities are unknown (see Section 3.2 for details).

Before proceeding with a description of the algorithm implementing the above bootstrap idea, we illustrate its capability using a data example. Figure 1 shows the monthly sea surface temperatures for the last three years (analyzed in Section 6) together with 1,000 bootstrap replications obtained when  $k = 1$  and using the bootstrap algorithm described in Section 3.2. Notice the asymmetric features of the time series paths generated as well as the fact that all 1,000 bootstrap samples displayed pass through the same final curve. That is, all generated bootstrap functional time series satisfy condition (11), which for the case  $k = 1$  reduces to  $\mathcal{X}_n^* = \mathcal{X}_n$ .

## 3.2 Bootstrap Algorithm

We now proceed with a detailed description of the bootstrap algorithm used to generate the functional pseudo-time series  $\mathcal{X}_1^*, \mathcal{X}_2^*, \dots, \mathcal{X}_n^*$  and  $\mathcal{X}_{n+1}^*$ . In the following algorithm, Steps 1 to 3 concern the generation of the future pseudo-element  $\mathcal{X}_{n+1}^*$ , while Steps 4 to 6 involve the generation of  $\mathcal{X}_1^*, \dots, \mathcal{X}_n^*$ .

**Step 1:** Center the observed functional time series by calculating  $\mathcal{Y}_t = \mathcal{X}_t - \bar{\mathcal{X}}_n$ ,  $\bar{\mathcal{X}}_n = n^{-1} \sum_{t=1}^n \mathcal{X}_t$ .

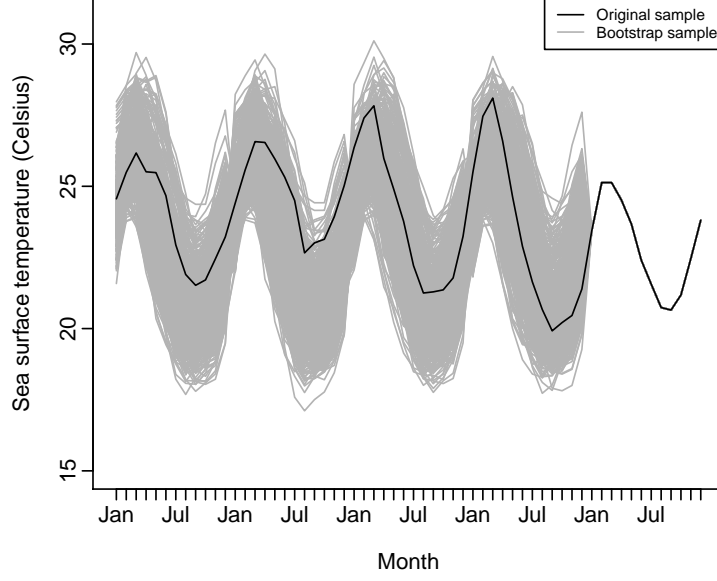


**Figure 1:** Sea surface temperature in El Niño region 1+2 displayed from January 2014 to December 2018 (black line) together with 1000 different bootstrap samples (gray lines) when  $k = 1$ .

**Step 2:** Select integers  $m$  and  $p$ , where  $m$  is the truncation number in (12) and  $p$  the order used to approximate the infinite-order vector autoregressive representations (7) and (8). Denote by  $(\hat{\xi}_1, \hat{\xi}_2, \dots, \hat{\xi}_n)$  the estimated  $m$ -dimensional vector of scores; that is,

$$\hat{\xi}_t = (\langle \mathcal{Y}_t, \hat{v}_j \rangle, j = 1, 2, \dots, m)^\top, \quad t = 1, 2, \dots, n$$

where  $\hat{v}_j, j = 1, 2, \dots, m$  are the estimated (up to a sign) orthonormal eigenfunctions corresponding to the  $m$  largest estimated eigenvalues of the lag-0 sample autocovariance operator  $\hat{C}_0 = n^{-1} \sum_{t=1}^n \mathcal{Y}_t \otimes \mathcal{Y}_t$ .

**Step 3:** Fit a VAR( $p$ ) process to the “forward” series of estimated scores; that is,

$$\hat{\xi}_t = \sum_{j=1}^p \hat{A}_{j,p} \hat{\xi}_{t-j} + \hat{e}_t, \quad t = p+1, p+2, \dots, n,$$

with  $\hat{e}_t$  being the residuals. Generate

$$\xi_{n+1}^* = \sum_{l=1}^{\min\{p,k\}} \hat{A}_{l,p} \hat{\xi}_{n+1-l} + \sum_{l=\min\{p,k\}+1}^p \hat{A}_{l,p} \xi_{n+1-l}^* + e_{n+1}^*,$$

where the second sum is zero if  $p \leq k$  and  $e_{n+1}^*$  is i.i.d. resampled from the set of centered residuals  $\{\hat{e}_t - \bar{e}_n, t = p+1, p+2, \dots, n\}$ ,  $\bar{e}_n = (n-p)^{-1} \sum_{t=p+1}^n \hat{e}_t$ . Notice that the pseudo-scores  $\xi_{n+1-l}^*$  appearing in the second sum in the above displayed equation are those generated in Step 5 bellow. Calculate

$$\mathcal{X}_{n+1}^* = \bar{\mathcal{X}}_n + \sum_{j=1}^m \mathbf{1}_j^\top \xi_{n+1}^* \hat{v}_j + U_{n+1,m}^*,$$

where  $U_{n+1,m}^*$  is i.i.d. resampled from the set  $\{\hat{U}_{t,m} - \bar{U}_n, t = 1, 2, \dots, n\}$ ,  $\bar{U}_n = n^{-1} \sum_{t=1}^n \hat{U}_{t,m}$  and  $\hat{U}_{t,m} = \mathcal{Y}_t - \sum_{j=1}^m \mathbf{1}_j' \hat{\xi}_t \hat{v}_j$ . Recall that  $\mathbf{1}_j$  denotes the  $d$ -dimensional vector with the  $j^{\text{th}}$  component equal to 1 and 0 elsewhere.

If  $p \leq k$ , move to Step 4. If  $p > k$ , generate for  $l = 1, 2, \dots, p-k$  additional random vectors  $\xi_{n+l}^* = \sum_{j=1}^p \hat{A}_{j,p} \xi_{n+l-j}^* + e_{n+l}^+$ , where we set  $\xi_t^* = \hat{\xi}_t$  for  $t \leq n$  and  $e_{n+l}^+$  are i.i.d. generated as  $e_{n+1}^*$ .

**Step 4:** Fit a VAR( $p$ ) process to the “backward” series of estimated scores; that is,

$$\hat{\xi}_t = \sum_{j=1}^p \hat{B}_{j,p} \hat{\xi}_{t+j} + \hat{v}_t, \quad t = 1, 2, \dots, n-p.$$

**Step 5:** Generate a pseudo-time series of the scores  $\{\xi_1^*, \xi_2^*, \dots, \xi_n^*\}$  by setting

$$\xi_t^* = \hat{\xi}_t, \quad \text{for } t = n, n-1, \dots, n-k+1$$

and using the backward vector autoregression

$$\xi_t^* = \sum_{j=1}^p \hat{B}_{j,p} \xi_{t+j}^* + v_t^*, \quad \text{for } t = n-k, n-k-1, \dots, 1.$$

Here  $v_1^*, v_2^*, \dots, v_{n-k}^*$  are obtained as (see (10))

$$v_t^* = \hat{B}_p(L^{-1}) \hat{A}_p^{-1}(L) e_t^*,$$

with  $\hat{A}_p(z) = I - \sum_{j=1}^p \hat{A}_{j,p} z^j$ ,  $\hat{B}_p(z) = I - \sum_{j=1}^p \hat{B}_{j,p} z^j$ ,  $z \in \mathcal{C}$ , and where the  $e_t^*$  are i.i.d.

resampled as in Step 3.

**Step 6:** Generate a pseudo-functional time series  $\{\mathcal{X}_1^*, \mathcal{X}_2^*, \dots, \mathcal{X}_n^*\}$  as follows. For  $t = n, n-1, \dots, n-k+1$  set

$$\begin{aligned}\mathcal{X}_t^* &= \bar{\mathcal{X}}_n + \sum_{j=1}^m \mathbf{1}_j^\top \hat{\boldsymbol{\xi}}_t \hat{v}_j + \hat{U}_{t,m} \\ &\equiv \mathcal{X}_t,\end{aligned}$$

while for  $t = n-k, t = n-k-1, \dots, 1$ , use the obtained backward pseudo-scores  $\boldsymbol{\xi}_1^*, \boldsymbol{\xi}_2^*, \dots, \boldsymbol{\xi}_{n-k}^*$  and calculate

$$\mathcal{X}_t^* = \bar{\mathcal{X}}_n + \sum_{j=1}^m \mathbf{1}_j^\top \boldsymbol{\xi}_t^* \hat{v}_j + U_{t,m}^*.$$

Here, the  $U_{t,m}^*$  are i.i.d. pseudo-elements resampled as in Step 3.

**Step 7:** Using  $(\mathcal{X}_1^*, \mathcal{X}_2^*, \dots, \mathcal{X}_n^*)$ , fit the “model” applied to perform the prediction  $\hat{\mathcal{X}}_{n+1}$  and calculate the pseudo-predictor

$$\hat{\mathcal{X}}_{n+1}^* = \bar{\mathcal{X}}_n + \hat{g}^* (\mathcal{X}_n - \bar{\mathcal{X}}_n, \mathcal{X}_{n-1} - \bar{\mathcal{X}}_n, \dots, \mathcal{X}_{n-k+1} - \bar{\mathcal{X}}_n), \quad (13)$$

where  $\hat{g}^*$  is the same estimator as  $\hat{g}$  but obtained using the pseudo-time series  $\mathcal{X}_1^*, \mathcal{X}_2^*, \dots, \mathcal{X}_n^*$ .

**Step 8:** Use the distribution of  $\mathcal{E}_{n+1}^* = \mathcal{X}_{n+1}^* - \hat{\mathcal{X}}_{n+1}^*$  to approximate the conditional distribution of  $\mathcal{E}_{n+1} = \mathcal{X}_{n+1} - \hat{\mathcal{X}}_{n+1}$  given  $\mathcal{X}_{n-k+1}, \mathcal{X}_{n-k+2}, \dots, \mathcal{X}_n$ .

Before investigating the theoretical properties of the above bootstrap procedure and its practical use for the construction of prediction intervals and prediction bands, some remarks are in order.

Notice that  $\mathcal{X}_{n+1}^*$  in Step 3 is generated in a model-free way, while the estimated model  $\hat{g}^*$  is only used for obtaining the pseudo-predictor  $\hat{\mathcal{X}}_{n+1}^*$ . In this way the pseudo-error  $\mathcal{X}_{n+1}^* - \hat{\mathcal{X}}_{n+1}^*$  imitates not only the innovation and estimation errors affecting the prediction error  $\mathcal{X}_{n+1} - \hat{\mathcal{X}}_{n+1}$  but also the error arising from possible model misspecification. In Steps 4 and 5, the backward

vector autoregressive representation is used to generate the pseudo-time series of scores  $\xi_t^*$ ,  $t = 1, 2, \dots, n$ , where this time series satisfies the condition  $\xi_t^* = \hat{\xi}_t$  for  $t = n - k + 1, n - k + 2, \dots, n$ . This enables the generation of a functional pseudo-time series  $\mathcal{X}_1^*, \mathcal{X}_2^*, \dots, \mathcal{X}_n^*$  in Step 6, satisfying requirement (11). A problem occurs when  $p > k$ , that is, when the autoregressive order used is larger than the number of past functional observations involved in calculating the predictor  $\hat{\mathcal{X}}_{n+1}$ . In this case and to appropriately run the backward vector autoregression, the time series of scores must be extended with the  $p - k$  “missing” scores, that is, with the scores  $\xi_t$  for  $t = n + 1, n + 2, \dots, n + p - k$ . This particular problem is solved in Step 3 by generating the pseudo-scores  $\xi_{n+1}^*$ , for  $l = 1, 2, \dots, n + p - k$ .

### 3.3 Bootstrap Validity

We establish consistency of the proposed bootstrap procedure in approximating the conditional error distribution (5) of interest. Regarding the underlying class of functional processes, we assume throughout this paper that  $\mathbf{X}$  is a purely non-deterministic, mean square continuous, and  $L^4$ - $\mathcal{M}$  approximable. The mean square continuity of the process  $\mathbf{X}$  implies that its mean and covariance functions are continuous. For simplicity of notation, we assume that  $E\mathcal{X}_t = 0$ . The  $L^4$ - $\mathcal{M}$  approximability property allows for a weak dependence structure of the underlying functional process, which covers a wide range of commonly used functional time series models, including functional linear processes and functional autoregressive conditional heteroscedasticity process (see [Hörmann and Kokoszka, 2010](#), for details).

Because we condition on the last  $k$  observations, in what follows, all asymptotic results are derived under the assumption that we have observed a functional time series  $X_s, X_{s+1}, \dots, X_n$  in which we view  $n$  as fixed and allow  $s \rightarrow -\infty$ . This is also the meaning of the statement “as  $n \rightarrow \infty$ ” used in all derivations and asymptotic considerations in the sequel. Some conditions regarding the underlying process  $\mathbf{X}$  and the behavior of the bootstrap parameters  $m$  and  $p$  as well as the estimates  $\hat{g}$  and  $\hat{g}^*$  used are first imposed. Notice that to achieve bootstrap consistency, it is necessary to allow not only for the order  $p$  of the fitted autoregression but also for the dimension  $m$  of the number of principal components used to increase to infinity with the sample size. This is required to enable the bootstrap to appropriately capture both the entire



temporal dependence structure of the vector process of scores and the infinite dimensional structure of the prediction error  $\mathcal{E}_{n+1}$ .

**Assumption 1:**

- (i) The autocovariance operator  $C_h$  of  $\mathbf{X}$  satisfies  $\sum_{h \in \mathbb{Z}} |h| \|C_h\|_{HS} < \infty$ .
- (ii) For all  $\omega \in [0, \pi]$ , the spectral density operator  $\mathcal{F}_\omega$  is of full rank, that is,  $\text{kern}(\mathcal{F}_\omega) = 0$  and the eigenvalues  $\lambda_j$  of the full rank covariance operator  $\mathcal{C}_0$  (in descending order) are denoted by  $\lambda_1 > \lambda_2 > \lambda_3 > \dots > 0$ .

**Assumption 2:** The sequences  $p = p(n)$  and  $m = m(n)$  satisfy  $p \rightarrow \infty$  and  $m \rightarrow \infty$ , as  $n \rightarrow \infty$ , such that

- (i)  $m^2 / \sqrt{p} \rightarrow 0$ ,
- (ii)  $\frac{p^3}{\sqrt{nm}\lambda_m^2} \sqrt{\sum_{j=1}^m \alpha_j^{-2}} = O(1)$ , where  $\alpha_1 = \lambda_1 - \lambda_2$  and  $\alpha_j = \min\{\lambda_{j-1} - \lambda_j, \lambda_j - \lambda_{j+1}\}$  for  $j = 2, 3, \dots, m$ .
- (iii)  $m^4 p^2 \sum_{j=1}^p \|\tilde{A}_{j,p} - A_{j,p}\|_F = O_P(1)$ , where  $\|A\|_F$  denotes the Frobenius norm of the matrix  $A$ ,  $\tilde{A}_{j,p}, j = 1, 2, \dots, p$  are the same estimators as  $\hat{A}_{j,p}, j = 1, 2, \dots, p$ , but based on the time series of true scores  $\xi_1, \xi_2, \dots, \xi_n$  and  $(A_{1,p}, A_{2,p}, \dots, A_{p,p})$  are the coefficient matrices of the best (in the mean square sense) linear predictor of  $\xi_t$  based on the finite past  $\xi_{t-1}, \xi_{t-2}, \dots, \xi_{t-p}$ .

**Assumption 3:** The estimators  $\hat{g}$  and  $\hat{g}^*$  converge to the same limit  $g_0$ ; that is,  $\|\hat{g} - g_0\|_{\mathcal{L}} = o_P(1)$  and  $\|\hat{g}^* - g_0\|_{\mathcal{L}} = o_P(1)$ , where  $\|\cdot\|_{\mathcal{L}}$  denotes the operator norm.

Some comments on the above assumptions are in order. Assumption 1(i) implies that  $\mathcal{F}_\omega$  is a continuously differentiable function of the frequency  $\omega$ . Allowing for the number of  $m$  principal components used to increase to infinity makes the asymptotic analysis for establishing bootstrap validity relatively involved. This is because the rate of increase of  $m$  to infinity should take into account the fact that the bootstrap procedure is based on the estimated instead the actual time series of scores, and that the dimension and the order of the fitted vector autoregression increases to infinity as  $n$  increases to infinity. Further, the positive lower bound of the spectral density matrix  $f_\xi(\omega)$  of the scores approaches zero as the dimension  $m$  of the

vector  $\xi_t$  increases. This is true because the eigenvalues  $v_j(\omega)$  of the trace class spectral density operator  $\mathcal{F}_\omega$ , approach zero as  $j \rightarrow \infty$  for all  $\omega \in [0, \pi]$ . Assumption 2 summarizes the technical conditions needed for the rate at which  $m$  and  $p$  increase to infinity with  $n$  in order to balance these different effects on the asymptotic consistency of the bootstrap.

Given that we do not focus on a specific predictor, Assumption 3 is necessarily a high-level type assumption. It requires that the estimator  $\hat{g}^*$ , which is based on the bootstrap pseudo-time series  $\mathcal{X}_1^*, \mathcal{X}_2^*, \dots, \mathcal{X}_n^*$ , converges in the operator norm, to the same limit  $g_0$  as the estimator  $\hat{g}$  based on the time series  $\mathcal{X}_1, \mathcal{X}_2, \dots, \mathcal{X}_n$ . Notice that Assumption 3 can only be verified in a case-by-case investigation and for a specific operator  $g$  at hand and with its particular estimators  $\hat{g}$  and  $\hat{g}^*$ , respectively, used to perform the prediction.

To elaborate, consider the following example. Suppose that a FAR(1) model  $\mathcal{X}_t = \Phi(\mathcal{X}_{t-1}) + \varepsilon_t$  is used in equations (4) and (13) to obtain the predictors  $\hat{\mathcal{X}}_{n+1}$  and  $\hat{\mathcal{X}}_{n+1}^*$ , respectively. A common estimator of  $\Phi$  based on an approximative solution of the Yule-Walker-type equation  $C_1 = \Phi C_0$ , is given by

$$\hat{\Phi}_M(\cdot) = \frac{1}{n-1} \sum_{t=1}^{n-1} \sum_{i=1}^M \sum_{j=1}^M \frac{1}{\hat{\lambda}_j} \langle \cdot, \hat{v}_j \rangle \langle \mathcal{X}_t, \hat{v}_j \rangle \langle \mathcal{X}_{t+1}, \hat{v}_i \rangle \hat{v}_i, \quad (14)$$

where  $M$  is some integer referring to the number of functional principal components included in the estimation of  $\Phi$  (Bosq, 2000; Hörmann and Kokoszka, 2012). Notice that in this example,  $\hat{g} = \hat{\Phi}_M$ . Now, for a fixed  $M$ , it is not difficult to show that  $\|\hat{\Phi}_M(\cdot) - g_0\|_{\mathcal{L}} \xrightarrow{P} 0$ , as  $s \rightarrow -\infty$ , where the limiting operator  $g_0$  is given by

$$g_0(\cdot) \equiv C_{1,M} \left( \sum_{j=1}^M \frac{1}{\lambda_j} \langle \cdot, v_j \rangle v_j \right). \quad (15)$$

Here,  $C_{1,M}(\cdot) = E \langle \mathcal{X}_{t,M}, \cdot \rangle \mathcal{X}_{t+1,M}$  is an approximation of the lag-1 autocovariance operator  $C_1$  (see Equation (12) for the definition of  $\mathcal{X}_{t,M}$ ). Further,  $\sum_{j=1}^M \lambda_j^{-1} \langle \cdot, v_j \rangle v_j$  is the corresponding approximation of the inverse operator  $C_0^{-1}(\cdot) = \sum_{j=1}^{\infty} \lambda_j^{-1} \langle \cdot, v_j \rangle v_j$ , which appears when solving the aforementioned Yule-Walker-type equation (see Horváth and Kokoszka, 2012, Chapter 13, for details). Similarly, it is not difficult to show that the same convergence also is true for the bootstrap estimator  $\hat{g}_0^*$ , that is,  $\|\hat{g}_0^* - g_0\|_{\mathcal{L}} \xrightarrow{P} 0$ . However, if interest is focused on

consistently estimating the operator  $\Phi$ , then, from an asymptotic perspective, the number  $M$  of functional principal components used in approximating the inverse of the operator  $C_0$  and that are involved in the estimator  $\widehat{\Phi}_M$  has to increase at an appropriate rate to infinity as  $n$  goes to infinity. In this case, it is well known that under certain regularity conditions, we obtain  $\|\widehat{\Phi}_M - \Phi\|_{\mathcal{L}} = o_P(1)$  (see [Bosq, 2000](#), Theorem 8.7). That is, in this case  $g_0 = \Phi$ , and this limit is different from the one given in (15). In such a case, and for the estimator  $\widehat{g}^*$  to also converge to the same limit, additional investigations are needed since the technical derivations are more involved compared to the case of a fixed  $M$ ; (see [Paparoditis, 2018](#), for these types of asymptotic considerations).

Before stating our first consistency result, we fix some additional notation. Let  $\mathcal{X}_{n,k} = (\mathcal{X}_n, \mathcal{X}_{n-1}, \dots, \mathcal{X}_{n-k+1})$ , and denote by  $\mathcal{C}_{\mathcal{E}}$  and  $\mathcal{C}_{\mathcal{E}}^*$  the conditional covariance operators of the random elements  $\mathcal{E}_{n+1}$  and  $\mathcal{E}_{n+1}^*$ , respectively, given  $\mathcal{X}_{n,k}$ . That is,  $\mathcal{C}_{\mathcal{E}} = E(\mathcal{E}_{n+1} \otimes \mathcal{E}_{n+1} | \mathcal{X}_{n,k})$  and  $\mathcal{C}_{\mathcal{E}}^* = E^*(\mathcal{E}_{n+1}^* \otimes \mathcal{E}_{n+1}^* | \mathcal{X}_{n,k})$ . Recall that  $\mathcal{X}_t^* = \mathcal{X}_t$  for  $t = n, n-1, \dots, n-k+1$ . Further, let

$$\sigma_{n+1}^2(\tau) = c_{\mathcal{E}}(\tau, \tau) \text{ and } \sigma_{n+1}^{*2}(\tau) = c_{\mathcal{E}}^*(\tau, \tau), \quad \tau \in [0, 1],$$

where  $c_{\mathcal{E}}$  and  $c_{\mathcal{E}}^*$  denote the kernels of the conditional covariance (integral) operators  $\mathcal{C}_{\mathcal{E}}$  and  $\mathcal{C}_{\mathcal{E}}^*$ , respectively. Denote by  $\mathcal{L}_{\mathcal{X}_{n,k}}(\mathcal{E}_{n+1})$  the conditional distribution  $\mathcal{E}_{n+1} | \mathcal{X}_{n,k}$ , and by  $\mathcal{L}_{\mathcal{X}_{n,k}}(\mathcal{E}_{n+1}^* | X_1, X_2, \dots, X_n)$  the conditional distribution  $\mathcal{E}_{n+1}^* | \mathcal{X}_{n,k}$ , given the observed functional time series  $\mathcal{X}_1, \mathcal{X}_2, \dots, \mathcal{X}_n$ . The following theorem establishes consistency of the bootstrap procedure in estimating the conditional distribution of interest.

**Theorem 3.1** *Suppose that Assumptions 1, 2, and 3 are satisfied. Then,*

$$d\left(\mathcal{L}_{\mathcal{X}_{n,k}}(\mathcal{E}_{n+1}), \mathcal{L}_{\mathcal{X}_{n,k}}(\mathcal{E}_{n+1}^* | \mathcal{X}_1, \mathcal{X}_2, \dots, X_n)\right) = o_P(1), \quad (16)$$

where  $d$  is any metric metricizing weak convergence on  $\mathcal{H}$ .

The above result, together with the continuous mapping theorem, allows for the use of the conditional distribution of  $\mathcal{E}_{n+1}^*(\tau)$  to construct pointwise prediction intervals for  $\mathcal{X}_{n+1}(\tau)$  or for the use of the conditional distribution of  $\sup_{\tau \in [0,1]} |\mathcal{E}_{n+1}^*(\tau)|$  to construct prediction bands for  $\mathcal{X}_{n+1}$ . However, the latter prediction bands will have the same width for all values of  $\tau \in [0, 1]$

because they will not appropriately reflect the local variability of the prediction error  $\mathcal{E}_{n+1}(\tau)$ . One way to take this variability into account is to use the studentized conditional distribution of the prediction error, that is to consider the process  $\{\mathcal{E}_{n+1}(\tau)/\sigma_{n+1}(\tau), \tau \in [0, 1]\}$  on  $\mathcal{H}$  to construct prediction bands. However, in this case, and additional to the weak convergence of  $\mathcal{E}_{n+1}^*$  to  $\mathcal{E}_{n+1}$  on  $\mathcal{H}$ , establishing bootstrap consistency requires the uniform (over  $\tau \in [0, 1]$ ) convergence of the conditional variance of the prediction error  $\sigma_{n+1}^{*2}(\tau)$  against  $\sigma_{n+1}^2(\tau)$ . This will allow for the proposed bootstrap procedure to appropriately approximate the random behavior of the studentized process  $\{\mathcal{E}_{n+1}(\tau)/\sigma_{n+1}(\tau), \tau \in [0, 1]\}$  on  $\mathcal{H}$ . To achieve such a uniform consistency of bootstrap estimates, some additional conditions compared to those stated in the previous Assumptions 2 and 3 are needed. The following is the modification of Assumption 2 needed.

**Assumption 2'**: The sequences  $m = m(n)$  and  $p = p(n)$  satisfy Assumptions 2 (i), (iii), and

$$(ii) \quad \frac{p^5 m}{n^{1/2} \lambda_m^{5/2}} \sqrt{\sum_{j=1}^m \alpha_j^{-2}} = O(1).$$

Our next assumption imposes additional conditions to those made in Assumption 3 on the consistency properties of the estimators  $\widehat{g}$  and  $\widehat{g}^*$ .

**Assumption 3'**: The estimators  $\widehat{g}(x)$  and  $\widehat{g}^*(x)$  converge to the same limit  $g_0(x)$  for every  $x \in \mathcal{H}$  in the sense that  $\sup_{\tau \in [0, 1]} E \|\widehat{g}(x)(\tau) - g_0(x)(\tau)\|_2^2 \rightarrow 0$  and  $\sup_{\tau \in [0, 1]} E^* \|\widehat{g}^*(x)(\tau) - g_0(x)(\tau)\|_2^2 \rightarrow 0$  in probability.

We can now establish the next theorem, which states the desired weak convergence of  $\mathcal{L}_{\mathcal{X}_{n,k}}(\mathcal{E}_{n+1}^*)$  given  $\mathcal{X}_1, \mathcal{X}_2, \dots, \mathcal{X}_n$ , as well as the uniform convergence of the conditional variance function  $\sigma_{n+1}^{*2}(\cdot)$  of the bootstrap prediction error.

**Theorem 3.2** *Suppose that Assumption 1, 2' and 3' are satisfied. Then, additional to assertion (16) of Theorem 3.1, the following also is true:*

$$\sup_{\tau \in [0, 1]} \left| \sigma_{n+1}^{*2}(\tau) - \sigma_{n+1}^2(\tau) \right| \rightarrow 0, \text{ in probability.} \quad (17)$$

Theorem 3.2 and Slutsky's theorem theoretically justify the use of the bootstrap process  $\{\mathcal{E}_{n+1}^*(\tau) / \sigma_{n+1}^*(\tau), \tau \in [0, 1]\}$  to approximate the behavior of the process  $\{\mathcal{E}_{n+1}(\tau) / \sigma_{n+1}(\tau), \tau \in [0, 1]\}$ .

$[0, 1]\}$ . As the following corollary shows, this property of the bootstrap can successfully be used for the construction of simultaneous prediction bands for  $\mathcal{X}_{n+1}$  that appropriately account for the local variability of the prediction error distribution.

**Corollary 3.1** *Suppose that the assumptions of Theorem 3.2 are satisfied. For  $\tau \in [0, 1]$ , let*

$$V_{n+1}(\tau) = \frac{\mathcal{X}_{n+1}(\tau) - \hat{\mathcal{X}}_{n+1}(\tau)}{\sigma_{n+1}(\tau)}, \text{ and } V_{n+1}^*(\tau) = \frac{\mathcal{X}_{n+1}^*(\tau) - \hat{\mathcal{X}}_{n+1}^*(\tau)}{\sigma_{n+1}^*(\tau)}.$$

Then,

$$\sup_{x \in \mathbb{R}} \left| P \left( \sup_{\tau \in [0, 1]} |V_{n+1}(\tau)| \leq x \mid \mathcal{X}_{n,k} \right) - P^* \left( \sup_{\tau \in [0, 1]} |V_{n+1}^*(\tau)| \leq x \mid \mathcal{X}_{n,k} \right) \right| \rightarrow 0,$$

in probability, where  $P^*(A)$  denotes the probability of the event  $A$  given the functional time series  $\mathcal{X}_1, \mathcal{X}_2, \dots, \mathcal{X}_n$ .

## 4 Practical Construction of Prediction Intervals

As mentioned, the theoretical results of the previous section allow for the use of the quantiles of the distribution of  $\mathcal{E}_{n+1}^*(\tau)$  or of  $V_{n+1}^*(\tau)$  to construct pointwise prediction intervals for  $\mathcal{X}_{n+1}(\tau)$  or simultaneous prediction bands for  $\{\mathcal{X}_{n+1}(\tau), \tau \in [0, 1]\}$ . Notice that the conditional distribution of  $\mathcal{E}_{n+1}^*(\tau)$  can be estimated by Monte Carlo, that is, by generating  $B$  replicates of  $\mathcal{E}_{n+1}^*$  and  $\sigma_{n+1}^*$ , say,  $\mathcal{E}_{n+1,1}^*, \mathcal{E}_{n+1,2}^*, \dots, \mathcal{E}_{n+1,B}^*$  and  $\sigma_{n+1,1}^*, \sigma_{n+1,2}^*, \dots, \sigma_{n+1,B}^*$ . The empirical distribution of the pseudo-prediction errors  $\mathcal{E}_{n+1,b}^*(\tau)$  and  $V_{n+1,b}^*(\tau) = \mathcal{E}_{n+1,b}^*(\tau) / \sigma_{n+1,b}^*(\tau)$ ,  $b = 1, 2, \dots, B$ , can then be used to estimate the unknown conditional distributions of  $\mathcal{E}_{n+1}^*(\tau)$  and of  $V_{n+1}^*(\tau)$ .

More specifically, consider the important case in which each  $\mathcal{X}_t$  has been observed on a finite grid of points  $\tau_1, \tau_2, \dots, \tau_J$  in  $[0, 1]$  and that we have Monte Carlo estimates of the quantiles of the conditional distribution of  $\mathcal{E}_{n+1}^*(\tau_j)$ , say  $c_{\alpha/2}^*(\tau_j)$  and  $c_{1-\alpha/2}^*(\tau_j)$ ; that is,

$$P^*[c_{\alpha/2}^*(\tau_j) \leq \mathcal{E}_{n+1}^*(\tau_j) \leq c_{1-\alpha/2}^*(\tau_j)] = 1 - \alpha,$$

where  $1 - \alpha$  denotes the desired nominal coverage level. We can then construct a pointwise

prediction interval for  $\mathcal{X}_{n+1}(\tau_j)$  as

$$\left[ \widehat{\mathcal{X}}_{n+1}(\tau_j) + c_{\alpha/2}^*(\tau_j), \widehat{\mathcal{X}}_{n+1}(\tau_j) + c_{1-\alpha/2}^*(\tau_j) \right].$$

Pointwise prediction intervals can also be constructed using the bootstrap studentized prediction error  $V_{n+1}^*(\tau_j)$ ; that is,

$$\left[ \widehat{\mathcal{X}}_{n+1}(\tau_j) + \tau_{\alpha/2}^*(\tau_j) \sigma_{n+1}^*(\tau_j), \widehat{\mathcal{X}}_{n+1}(\tau_j) + \tau_{1-\alpha/2}^*(\tau_j) \sigma_{n+1}^*(\tau_j) \right].$$

where  $\tau_{\alpha/2}^*(\tau_j)$  and  $\tau_{1-\alpha/2}^*(\tau_j)$  are the corresponding quantiles of  $V_{n+1}^*(\tau_j)$ ; that is,

$$P \left[ \tau_{\alpha/2}^*(\tau_j) \leq V_{n+1}^*(\tau_j) \leq \tau_{1-\alpha/2}^*(\tau_j) \right] = 1 - \alpha.$$

The corresponding bootstrap simultaneous prediction band can then be calculated as follows. Let

$$M_n^* = \max_{1 \leq j \leq J} |V_{n+1}^*(\tau_j)|$$

and denote by  $M_{n,1-\alpha}^*$  the  $1 - \alpha$  quantile of the distribution of  $M_n^*$ , which can be estimated via Monte Carlo. A simultaneous  $(1 - \alpha)100\%$  prediction interval for  $\mathcal{X}_{n+1}$  over the grid of time points  $\tau_j, j = 1, 2, \dots, J$  is then given by

$$\left\{ \left[ \widehat{\mathcal{X}}_{n+1}(\tau_j) - M_{n,1-\alpha}^* \sigma_{n+1}^*(\tau_j), \widehat{\mathcal{X}}_{n+1}(\tau_j) + M_{n,1-\alpha}^* \sigma_{n+1}^*(\tau_j) \right], \quad j = 1, 2, \dots, J \right\}.$$

Note that by the theoretical results established in Section 3, all previously discussed prediction intervals achieve (asymptotically) the desired coverage probability.

## 5 Simulations

### 5.1 Choice of Tuning Parameters

Implementation of the proposed bootstrap procedure requires the choices of two tuning parameters: the VAR order  $p$  and the number  $m$  of functional principal components used. Several

approaches have been proposed in the literature to select these parameters (see [Paparoditis, 2018](#), for a discussion). To simplify calculations, in this paper, we apply simple and commonly used procedures to select these parameters. The number  $m$  of functional principal components is selected using the ratio of the total variance explained by the  $m$  principal components to the total variance of the random element  $\mathcal{X}_t$ . A standard rule is then used in this context, where  $m$  is selected as the smallest positive integer for which the empirical variance ratio satisfies

$$m_{n,Q} = \operatorname{argmin}_{j \geq 1} \left\{ \frac{\sum_{j=1}^m \hat{\lambda}_j}{\sum_{j=1}^n \hat{\lambda}_j} \geq Q \right\}.$$

Here  $\hat{\lambda}_s$  denotes the  $s^{\text{th}}$  estimated eigenvalue of the sample lag-0 covariance operator  $\hat{\mathcal{C}}_0$ , and  $Q$  is a pre-determined value, with  $Q = 0.85$  being a common choice (see, e.g., [Hörmann and Kokoszka, 2012](#), p.41). Once the dimension  $m$  of the score vector has been selected, the order  $p$  of the fitted VAR model is chosen using the corrected Akaike information criterion ([Hurvich and Tsai, 1993](#)), that is, by minimizing

$$\text{AICC}(p) = n \log |\hat{\Sigma}_{e,p}| + \frac{n(nm + pm^2)}{n - m(p + 1) - 1},$$

over a range of values of  $p$ . Here  $\hat{\Sigma}_{e,p} = n^{-1} \sum_{t=p+1}^n \hat{\mathbf{e}}_{t,p} \hat{\mathbf{e}}_{t,p}^\top$  and  $\hat{\mathbf{e}}_{t,p}$  are the residuals obtained by fitting a VAR( $p$ ) model (see also Step 3 of the bootstrap algorithm).

## 5.2 Simulation Study

We utilize Monte Carlo methods to investigate the finite sample performance of the proposed bootstrap procedure. The final goal of our simulation study is to evaluate the interval forecast accuracy of the bootstrap prediction intervals under both regimes, that is, when the model used for prediction coincides with the model generating the data and when this is not the case. To this end, we use a FAR(1) model for prediction. At the same time, we consider a data generating process, which allows us to investigate the behavior of the bootstrap method under the two regimes mentioned above. In particular, we generate functional time series

$\mathcal{X}_1, \mathcal{X}_2, \dots, \mathcal{X}_n$  according to

$$\mathcal{X}_t(\tau) = \int_0^1 \psi(\tau, s) \mathcal{X}_{t-1}(s) ds + b \cdot \mathcal{X}_{t-2}(\tau) + B_t(\tau), \quad t = 1, 2, \dots, n, \quad (18)$$

where  $\psi(\tau, s) = 0.34 \exp^{\frac{1}{2}(\tau^2 + s^2)}$ ,  $\tau \in [0, 1]$ , and  $B_t(\tau)$  are Brownian motions with zero mean and variance  $1/(L-1)$  with  $L = n+1$ . Notice that by the choice of the constants in the definition of the kernel function  $\psi$ , we have  $\|\Psi\|_{\mathcal{L}} \approx 0.5$ , where  $\Psi$  is the integral operator associated with the kernel  $\psi$ . Notice that for  $b = 0$  in (18), the data are generated by a FAR(1) model, while for  $b = 0.4$ , the data generating process follows a FAR(2) model, which is stationary because  $\|\Psi\|_{\mathcal{L}} + |b| < 1$ . We consider four sample sizes:  $n = 100, 200, 400$ , and  $800$ . Using the first 80% of the data as the initial training sample, we compute a one-step-ahead prediction interval. Then, we increase the training sample by one and compute the one-step-ahead prediction interval again. This procedure continues until the training sample reaches the sample size. With 20% of the data as the testing sample, we compute the interval forecast accuracy of the one-step-ahead prediction using the FAR(1) model.

### 5.3 Evaluation Criteria of the Interval Forecast Accuracy

To measure the interval forecast accuracy, we consider the coverage probability difference (CPD) between the nominal coverage probability and empirical coverage probability and the interval score criterion of [Gneiting and Raftery \(2007\)](#). The pointwise and uniform empirical coverage probabilities are defined as

$$\begin{aligned} \text{Coverage}_{\text{pointwise}} &= \frac{1}{n_{\text{test}} \times J} \sum_{\eta=1}^{n_{\text{test}}} \sum_{j=1}^J \left[ \mathbb{1}\{\mathcal{X}_{\eta}(\tau_j) < \hat{\mathcal{X}}_{\eta}^{\text{ub}}(\tau_j)\} + \mathbb{1}\{\mathcal{X}_{\eta}(\tau_j) > \hat{\mathcal{X}}_{\eta}^{\text{lb}}(\tau_j)\} \right], \\ \text{Coverage}_{\text{uniform}} &= \frac{1}{n_{\text{test}}} \sum_{\eta=1}^{n_{\text{test}}} [\mathbb{1}\{\mathcal{X}_{\eta}(\tau) < \hat{\mathcal{X}}_{\eta}^{\text{ub}}(\tau)\} + \mathbb{1}\{\mathcal{X}_{\eta}(\tau) > \hat{\mathcal{X}}_{\eta}^{\text{lb}}(\tau)\}], \end{aligned}$$

where  $n_{\text{test}}$  denotes the number of curves in the forecasting period,  $J$  denotes the number of discretized data points,  $\hat{\mathcal{X}}_{\eta}^{\text{ub}}$  and  $\hat{\mathcal{X}}_{\eta}^{\text{lb}}$  denote the upper and lower bounds of the corresponding prediction interval, and  $\mathbb{1}\{\cdot\}$  is the indicator function. The pointwise and uniform CPDs are



defined as

$$\text{CPD}_{\text{pointwise}} = \frac{1}{J} \sum_{j=1}^J |\text{Pointwise empirical coverage}(\tau_j) - \text{Nominal coverage}(\tau_j)|,$$

$$\text{CPD}_{\text{uniform}} = |\text{Uniform empirical coverage} - \text{Nominal coverage}|.$$

The smaller the CPD value, the better the performance of the forecasting method.

Another criterion for assessing pointwise interval forecast accuracy is the mean interval score introduced by [Gneiting and Raftery \(2007\)](#). The mean interval score, denoted by  $\bar{S}_\alpha$ , combines both CPD and half-width of pointwise prediction interval and it is defined as

$$\begin{aligned} \bar{S}_\alpha = \frac{1}{n_{\text{test}} \times J} \sum_{\eta=1}^{n_{\text{test}}} \sum_{j=1}^J \left\{ \left[ \hat{\mathcal{X}}_\eta^{\text{ub}}(\tau_j) - \hat{\mathcal{X}}_\eta^{\text{lb}}(\tau_j) \right] + \frac{2}{\alpha} \left[ \mathcal{X}_\eta(\tau_j) - \hat{\mathcal{X}}_\eta^{\text{ub}}(\tau_j) \right] \mathbb{1} \left[ \mathcal{X}_\eta(\tau_j) > \hat{\mathcal{X}}_\eta^{\text{ub}}(\tau_j) \right] \right. \\ \left. + \frac{2}{\alpha} \left[ \hat{\mathcal{X}}_\eta^{\text{lb}}(\tau_j) - \mathcal{X}_\eta(\tau_j) \right] \mathbb{1} \left[ \mathcal{X}_\eta(\tau_j) < \hat{\mathcal{X}}_\eta^{\text{lb}}(\tau_j) \right] \right\}, \end{aligned}$$

where  $\alpha$  denotes the level of coverage, customarily  $\alpha = 0.2$  corresponding to 80% prediction interval and  $\alpha = 0.05$  corresponding to 95% prediction interval. The optimal interval score is achieved when  $\mathcal{X}_\eta(\tau_j)$  lies between  $\hat{\mathcal{X}}_\eta^{\text{lb}}(\tau_j)$  and  $\hat{\mathcal{X}}_\eta^{\text{ub}}(\tau_j)$ , with the distance between the upper bound and lower bounds being minimal.

## 5.4 Simulation Results

As mentioned, throughout the simulations we use an estimated FAR(1) model to perform the prediction. The FAR(1) model is given by  $\mathcal{Y}_t = \Phi(\mathcal{Y}_{t-1}) + \epsilon_t$ , where  $\mathcal{Y}_t = \mathcal{X}_t - \mu$ . Based on the centered functional time series  $\mathcal{X}_1 - \bar{\mathcal{X}}_n, \mathcal{X}_2 - \bar{\mathcal{X}}_n, \dots, \mathcal{X}_n - \bar{\mathcal{X}}_n$ , the lag-0 and lag-1 autocovariance operators  $\mathcal{C}_0$  and  $\mathcal{C}_1$ , respectively, are estimated, and a regularized Yule-Walker-type estimator  $\hat{\Phi}$  of  $\Phi$  is obtained (see also (14)). The corresponding predictor of  $\mathcal{X}_{n+1}$  is then given by  $\hat{\mathcal{X}}_{n+1} = \bar{\mathcal{X}}_n + \hat{\Phi}(\mathcal{X}_n - \bar{\mathcal{X}}_n)$ . Table 1, which presents results based on 1,000 replications (i.e., a pseudo-random seed for each replication) and  $B = 1,000$  bootstrap repetitions, summarizes the finite sample performance of the proposed bootstrap method to construct pointwise prediction intervals and simultaneous prediction bands.

From this table some interesting observations can be made. First of all, the empirical coverage

**Table 1:** Empirical performance of the bootstrap prediction intervals and bands using the FAR(1) model to perform one-step-ahead predictions.

| Nominal coverage | Criterion                     | $n = 100$ |           | $n = 200$ |           | $n = 400$ |           | $n = 800$ |           |
|------------------|-------------------------------|-----------|-----------|-----------|-----------|-----------|-----------|-----------|-----------|
|                  |                               | $b = 0$   | $b = 0.4$ | $b = 0$   | $b = 0.4$ | $b = 0$   | $b = 0.4$ | $b = 0$   | $b = 0.4$ |
| 80%              | Coverage <sub>pointwise</sub> | 0.763     | 0.732     | 0.773     | 0.766     | 0.783     | 0.783     | 0.793     | 0.796     |
|                  | CPD <sub>pointwise</sub>      | 0.0566    | 0.0826    | 0.0452    | 0.0470    | 0.0266    | 0.0270    | 0.0167    | 0.0167    |
|                  | Coverage <sub>uniform</sub>   | 0.740     | 0.689     | 0.766     | 0.740     | 0.791     | 0.768     | 0.803     | 0.786     |
|                  | CPD <sub>uniform</sub>        | 0.0974    | 0.1310    | 0.0743    | 0.0769    | 0.0398    | 0.0474    | 0.0271    | 0.0293    |
|                  | $\bar{S}_{\alpha=0.2}$        | 2.5376    | 2.9503    | 2.5352    | 2.7701    | 2.4698    | 2.6735    | 2.4398    | 2.6144    |
| 95%              | Coverage <sub>pointwise</sub> | 0.914     | 0.887     | 0.919     | 0.910     | 0.928     | 0.923     | 0.933     | 0.930     |
|                  | CPD <sub>pointwise</sub>      | 0.0472    | 0.0667    | 0.0335    | 0.0408    | 0.0238    | 0.0280    | 0.0174    | 0.0201    |
|                  | Coverage <sub>uniform</sub>   | 0.902     | 0.856     | 0.918     | 0.899     | 0.927     | 0.913     | 0.936     | 0.924     |
|                  | CPD <sub>uniform</sub>        | 0.0638    | 0.1024    | 0.0582    | 0.0600    | 0.0303    | 0.0400    | 0.0185    | 0.0281    |
|                  | $\bar{S}_{\alpha=0.05}$       | 3.5719    | 4.4472    | 3.5338    | 3.9926    | 3.4253    | 3.7677    | 3.3558    | 3.6655    |

of the prediction intervals is good, even for the small sample sizes considered, and improves considerably as the sample size increases, moving quite close to the desired nominal coverage. This is true for both the pointwise prediction intervals and the simultaneous prediction bands considered and for both coverage levels used in the simulation study. Further, the  $\bar{S}_\alpha$  values are systematically larger for  $b = 0.4$  than for  $b = 0$ . As discussed in the introduction, this expected result is attributable to the fact that the model misspecification error occurring for  $b = 0.4$ , also causes an increase in the variability of the prediction error distribution, leading to prediction intervals that are wider than those for  $b = 0$ .

## 6 Empirical Data Analysis

For the two real-life data sets analyzed in this section we consider prediction using the FAR(1) model and the nonparametric forecasting method (NFR). The latter method is based on nonparametric estimation of the lag-1 conditional mean function  $g(\mathcal{X}_n) = E(\mathcal{X}_{n+1}|\mathcal{X}_n)$  (also see Section 2.1). Recall that  $g(\mathcal{X}_n)$  is the best predictor of  $\mathcal{X}_{n+1}$  based on  $\mathcal{X}_n$ , and that a data-driven estimation of  $g$  can be obtained using different nonparametric smoothing techniques. We refer to the functional Nadarya-Watson estimator (see, e.g., Masry, 2005; Ferraty and Vieu, 2006), the functional local linear estimator, Berlinet et al. (2011), the functional  $k$ -nearest neighbor estimator, Kudraszow and Vieu (2013), and the distance-based local linear estimator Boj et al. (2010), to name a few. Throughout the simulations, we use the Nadaraya-Watson estimator, which leads to the predictor  $\hat{\mathcal{X}}_{n+1} = \hat{g}(\mathcal{X}_n)$  and where  $\hat{g}$  is given by

$$\hat{g}(\mathcal{X}_n) = \frac{\sum_{t=2}^n K(d(\mathcal{X}_n, \mathcal{X}_{t-1})/h) \mathcal{X}_t}{\sum_{t=2}^n K(d(\mathcal{X}_n, \mathcal{X}_{t-1})/h)}.$$

In the above expression,  $K(\cdot)$  is the Gaussian kernel and  $h$  is bandwidth, which in our calculations has been obtained using a generalized cross-validation procedure.

In addition to the construction of prediction intervals, we also demonstrate how the proposed bootstrap method can be used to select the prediction method that performs best based on a user-specified criterion. In particular, as we have seen, the future random element  $\mathcal{X}_{n+1}^*$  is generated in a model-free way, so that the bootstrap prediction error  $\hat{\mathcal{X}}_{n+1}^* - \mathcal{X}_{n+1}^*$  correctly imitates

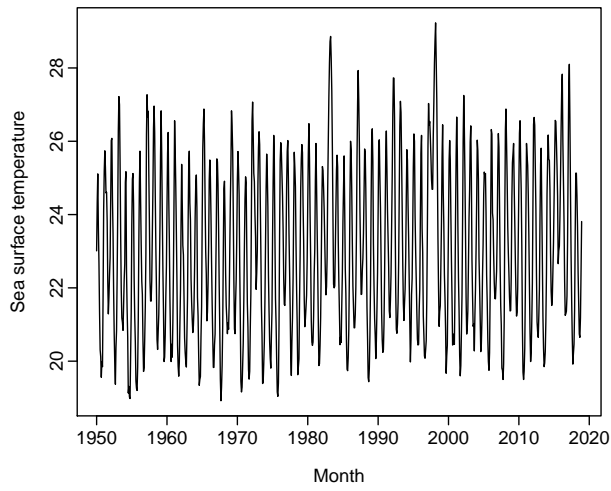
(asymptotically) the entire behavior of the prediction error  $\hat{\mathcal{X}}_{n+1} - \mathcal{X}_{n+1}$ , including the (possible) misspecification error arising from the particular model/method used to perform the prediction. Thus, using some loss  $L(\hat{\mathcal{X}}_{n+1}, \mathcal{X}_{n+1})$  and based on the behavior of the corresponding bootstrap loss  $L(\hat{\mathcal{X}}_{n+1}^*, \mathcal{X}_{n+1}^*)$ , the proposed bootstrap procedure can also be used to select the prediction method that performs better. In the following, we demonstrate such an application of the bootstrap in selecting between the FAR(1) and the NFR methods using the behavior of the bootstrap mean square prediction error  $E^*(\hat{\mathcal{X}}_{n+1}^*(\tau_j) - \mathcal{X}_{n+1}^*(\tau_j))^2, j = 1, 2, \dots, J$ , calculated for the two aforementioned competitive methods.

## 6.1 Monthly Sea Surface Temperature Data Set

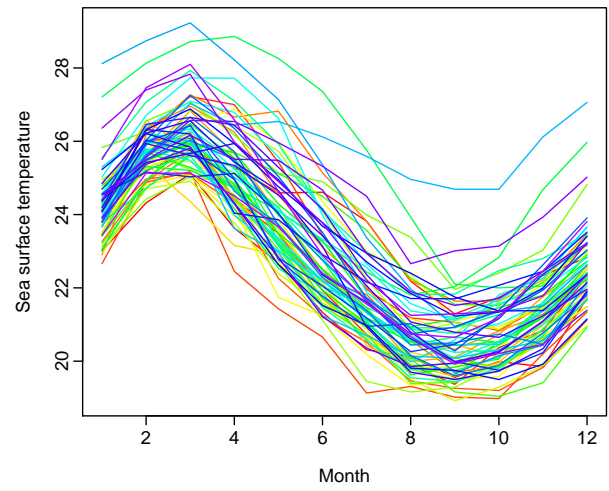
Let us consider the monthly sea surface temperatures from January 1950 to December 2018 available online at <https://www.cpc.ncep.noaa.gov/data/indices/ersst5.nino.mth.81-10.ascii>. These averaged sea surface temperatures were measured by moored buoys in the “Niño region”. We consider all four Niño regions: Niño 1+2 is defined by the coordinates  $0 - 10^\circ$  South,  $90 - 80^\circ$  West; Niño 3 is defined by the coordinates  $5^\circ$  North –  $5^\circ$  South,  $150^\circ - 90^\circ$  West; Niño 4 is defined by the coordinates  $5^\circ$  North –  $5^\circ$  South,  $160^\circ$  East –  $150^\circ$  West; Niño 3+4 is defined by the coordinates  $5^\circ$  North –  $5^\circ$  South,  $170 - 120^\circ$  West. For the sea surface temperatures in Niño 1+2 region, a univariate time series display is given in Figure 2a, with the same data shown in Figure 2b as a sliced functional time series.

Applying the proposed bootstrap procedure and the two compared forecasting methods, we generate a set of  $B = 1,000$  bootstrap one-step-ahead prediction error curves  $\mathcal{X}_{n+1}^* - \hat{\mathcal{X}}_{n+1}^*$ . These are presented in the left panel of Figure 3 for the FAR(1) predictor and in the right panel of the same figure for the NFR predictor.

In Figure 4, we present the bootstrap estimates of mean square error  $E(\hat{\mathcal{X}}_{n+1}(\tau_j) - \mathcal{X}_{n+1}(\tau_j))^2, j = 1, 2, \dots, J$  of the two prediction methods. As can clearly be seen in this figure, the mean square error produced by the NFR method is uniformly (over all points  $\tau_1, \tau_2, \dots, \tau_J$ ) smaller than the corresponding mean square prediction error produced using the FAR(1) method. Thus, for this functional time series, the use of the NFR method to perform the one step ahead prediction is recommended. The corresponding pointwise predictions intervals and simultaneous



(a) Univariate time series plot



(b) Functional time series plot

**Figure 2:** Time series (left panel) and rainbow plots (right panel) of sea surface temperatures in Niño 1+2 region from January 1982 to December 2017.

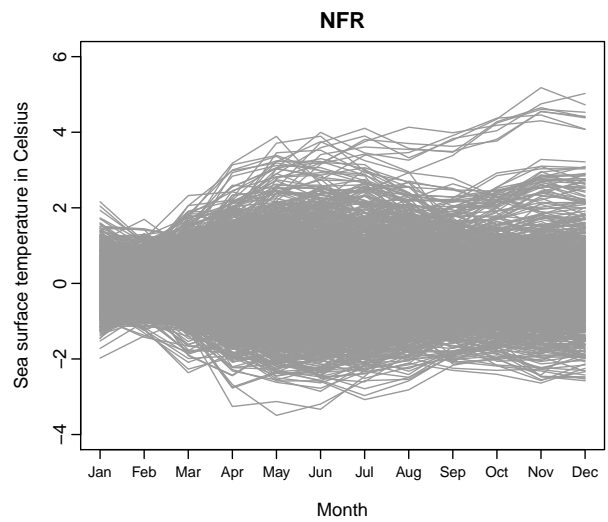
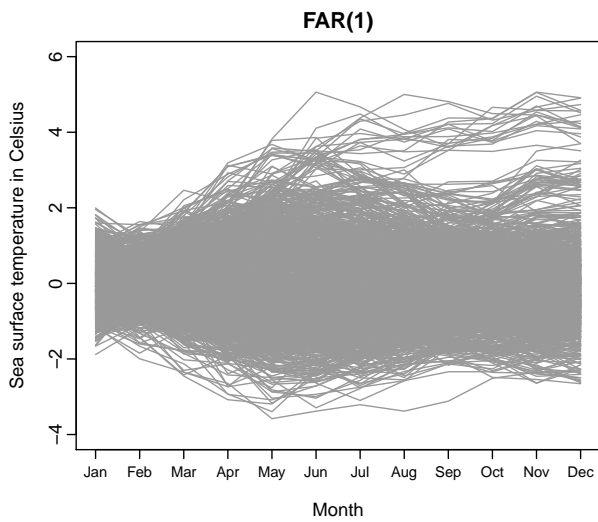


**Figure 3:** Bootstrap-generated one-step-ahead prediction error curves for the sea surface temperature data using the FAR(1) model (left panel) and the NFR method (right panel).

prediction bands are shown in Figure 4.

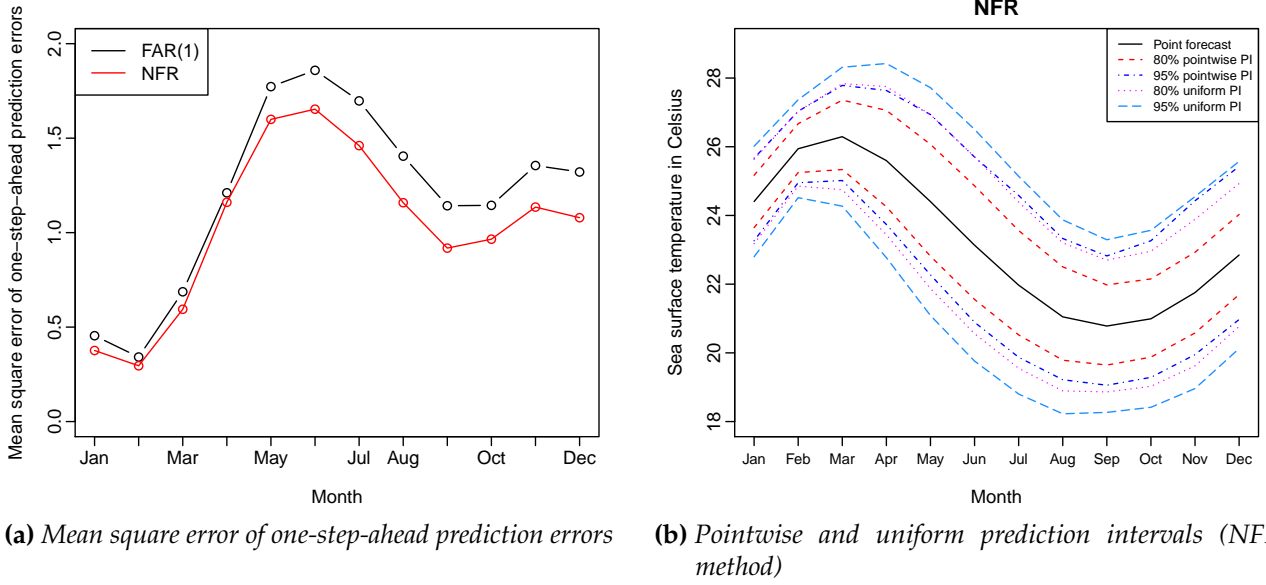


**Figure 4:** Bootstrap estimates of the mean square error of the one-step-ahead prediction for the FAR(1) model and the NFR method (left panel). Point forecast together with 80% and 95% pointwise and simultaneous nonparametric prediction intervals using the NFR method (right panel).

## 6.2 Intraday PM<sub>10</sub> Data Set

We analyze the half-hourly measurements of the concentration of particulate matter with an aerodynamic diameter of less than 10 $\mu$ m in ambient air taken in Graz, Austria, from October 1, 2010 to March 31, 2011. We convert  $N = 8,736$  discrete univariate time series points into  $n = 182$  daily curves. A univariate time series display of intraday pollution curves is given in Figure 5a, with the same data shown in Figure 5b as a time series of functions.

Using the bootstrap procedure, we generate  $B = 1,000$  functional pseudo-time series, and we apply the FAR(1) and the NFR forecasting methods to obtain a set of one-step-ahead prediction error curves. These are displayed in Figure 6. In the left panel of Figure 7, we show the bootstrap estimates of the mean square prediction error  $E(\hat{\mathcal{X}}_{n+1}(\tau_j) - \mathcal{X}_{n+1}(\tau_j))^2, j = 1, 2, \dots, J$ , obtained using the FAR(1) and NFR methods. As this figure shows, neither of the two methods is uniformly (i.e., over all points  $\tau_j \in [0, 1]$ ) better, with the FAR(1) method having an advantage. In particular, the root mean square error (RMSE) of the FAR(1) method is 1.451 compared with 2.054 of the NFR method. Therefore, we apply the FAR(1) method to perform the prediction for

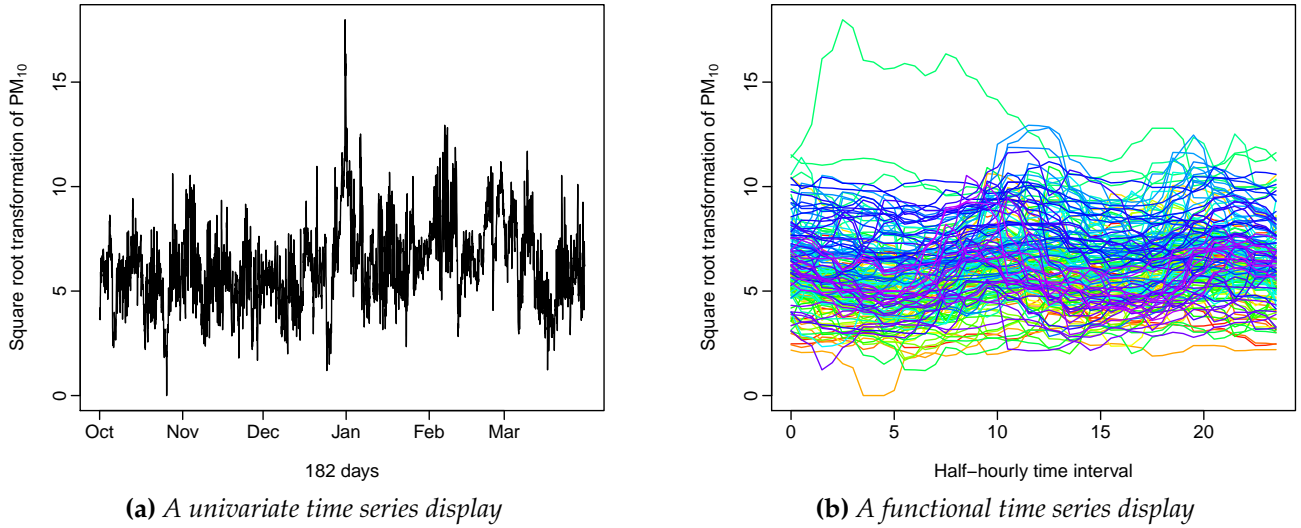


**Figure 5:** Graphical displays of intraday measurements of the  $PM_{10}$  from October 1, 2010 to March 31, 2011 in Graz, Austria.

this functional time series. The corresponding bootstrap-based pointwise prediction intervals and simultaneous prediction bands are displayed in the right panel of Figure 7.

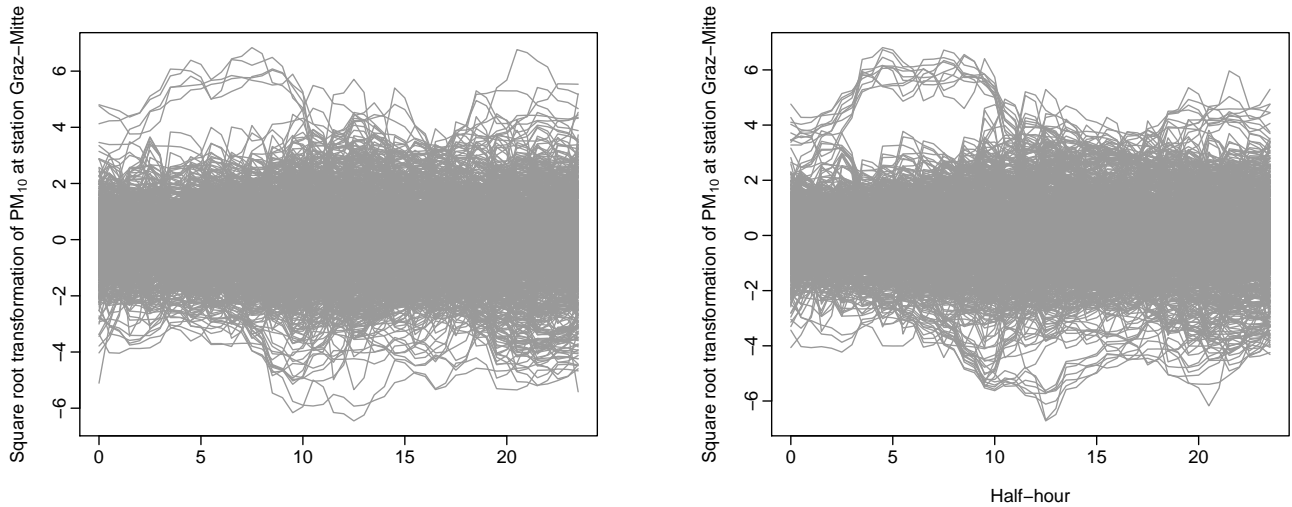


**Figure 6:** One-step-ahead prediction error curves for the intraday  $PM_{10}$  data using the FAR(1) model (left panel) and the NFR method (right panel).

In contrast with the relatively small sample size of  $n = 69$  curves of the Monthly Sea Surface Temperature data analyzed in the previous example, the moderate sample size of  $n = 182$  curves of the intraday  $PM_{10}$  data considered in this section, allows us to further evaluate the performance of the FAR(1) prediction method. For this, we use the observed data from October 1, 2010 to January 30, 2011 as the initial training sample, and we produce one-step-ahead

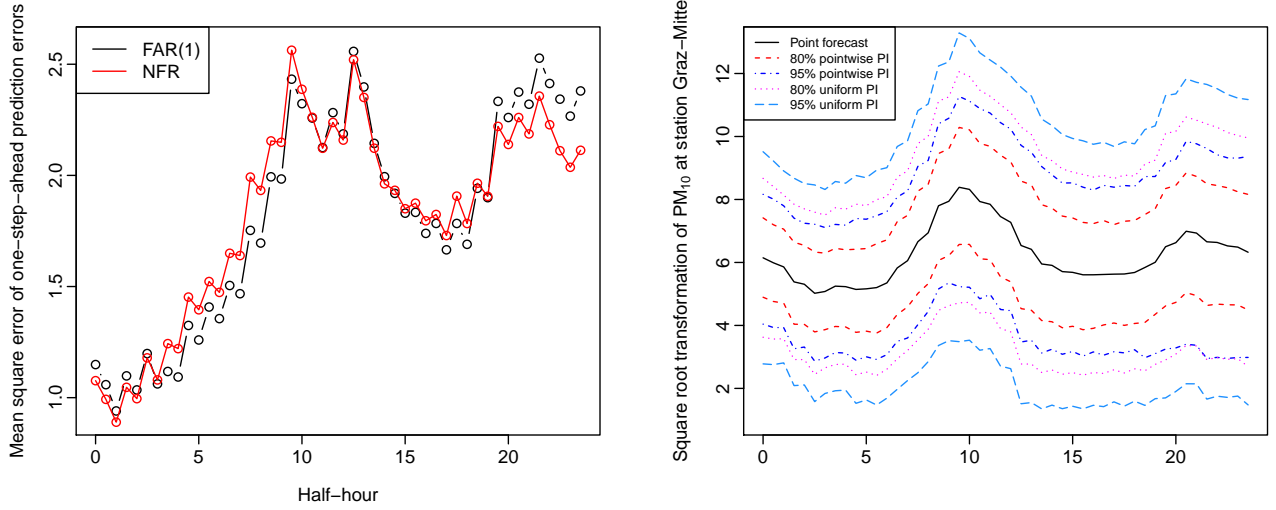


**Figure 7:** Bootstrap estimates of the mean square error of the one-step-ahead prediction for the FAR(1) model and the NFR method (left panel). Point forecast together with 80% and 95% pointwise and simultaneous nonparametric prediction intervals using the FAR(1) method (right panel).

forecasts by increasing the training sample by one curve each time. We iterate this procedure until the training sample contains all the observed data. In this way, we construct 60 one-step-ahead forecasts, enabling us to assess the forecast accuracy of the FAR(1) method. The results obtained are shown in Table 2.

**Table 2:** Evaluation of the interval forecast accuracy for the  $PM_{10}$  data set using the FAR(1) model for prediction and the bootstrap procedure with 1000 bootstrap replications.

| Nominal coverage | Criterion                |       |
|------------------|--------------------------|-------|
| 80%              | $CPD_{\text{pointwise}}$ | 0.789 |
|                  | $\bar{S}_{\alpha=0.2}$   | 5.189 |
|                  | $CPD_{\text{uniform}}$   | 0.833 |
| 95%              | $CPD_{\text{pointwise}}$ | 0.943 |
|                  | $\bar{S}_{\alpha=0.05}$  | 7.528 |
|                  | $CPD_{\text{uniform}}$   | 0.917 |

As seen in Table 2, the FAR(1) prediction performs well, and the proposed bootstrap method produces pointwise prediction intervals and simultaneous prediction bands, the empirical coverages of which are close to the desired nominal levels.



## 7 Conclusions

We have presented a novel bootstrap method for the construction of pointwise or simultaneous prediction intervals for a functional time series. Our method generates, in a model-free way, future functional pseudo-random elements that allow for valid estimation of the conditional distribution of the prediction error that a user-selected prediction method produces. The obtained bootstrap estimates of the prediction error distribution consider not only the innovation and the estimation errors associated with prediction but also the error arising from a different model being used for prediction than the one generating the observed functional time series. Theoretical results were presented to justify the use of the proposed bootstrap method in constructing pointwise prediction intervals and simultaneous prediction bands that appropriately consider the local variability of the conditional distribution of the prediction error. Through a series of simulations, we have demonstrated the good finite sample behavior of the bootstrap method presented. The two real-life data analyzed have demonstrated the capabilities and the good finite sample performance of the presented bootstrap method, not only in the construction of prediction intervals but also in selecting between different prediction models/methods the one that performs better.

## Acknowledgments

This research was initiated while the first author was visiting the Research School of Finance, Actuarial Studies and Statistics at the Australian National University in Canberra. He wishes to thank this institution for its great hospitality. The authors would like to thank the comments and suggestions received from the participants at the Fourth Conference of the International Society for Nonparametric Statistics and the Third Time Series and Forecasting Symposium held at the University of Sydney.

## Appendix A Proofs

Recall that  $\mathcal{X}_{n+1} = \sum_{j=1}^m \mathbf{1}_j^\top \boldsymbol{\xi}_{n+1} v_j + U_{n+1,m}$ ,  $\hat{\mathcal{X}}_{n+1} = \hat{g}(\mathcal{X}_n, \dots, \mathcal{X}_{n-k+1})$ ,  $\mathcal{X}_{n+1}^* = \sum_{j=1}^m \mathbf{1}_j^\top \boldsymbol{\xi}_{n+1}^* \hat{v}_j + U_{n+1,m}^*$  and  $\hat{\mathcal{X}}_{n+1}^* = \hat{g}^*(\mathcal{X}_n, \dots, \mathcal{X}_{n-k+1})$ . Define  $\mathcal{X}_{n+1,m}^+ = \sum_{j=1}^m \mathbf{1}_j^\top \boldsymbol{\xi}_{n+1}^+ v_j$ , where  $\boldsymbol{\xi}_{n+1}^+ = \sum_{j=1}^p \tilde{A}_{j,p} \boldsymbol{\xi}_{n+1-j} + \mathbf{e}_{n+1}^+$ , with  $\mathbf{e}_{n+1}^+$  i.i.d. resampled from the set  $\{\tilde{\mathbf{e}}_t - \bar{\tilde{\mathbf{e}}}_n, t = p+1, p+2, \dots, n\}$ ,  $\bar{\tilde{\mathbf{e}}}_n = (n-p)^{-1} \sum_{t=p+1}^n \tilde{\mathbf{e}}_t$ , and  $\tilde{\mathbf{e}}_t = \boldsymbol{\xi}_t - \sum_{j=1}^p \tilde{A}_{j,p} \boldsymbol{\xi}_{t-j}$ ,  $t = p+1, p+2, \dots, n$ , are the residuals obtained from an autoregressive fit based on the true scores  $\boldsymbol{\xi}_1, \boldsymbol{\xi}_2, \dots, \boldsymbol{\xi}_n$ . To simplify notation we set  $\boldsymbol{\xi}_{n+1}^* = \sum_{l=1}^p \hat{A}_{l,p} \hat{\boldsymbol{\xi}}_{n+1-l} + \mathbf{e}_{n+1}^*$ .

We first state the following lemma.

**Lemma A.1** *Let  $\Gamma_m(0) = E(\boldsymbol{\xi}_{n+1} \boldsymbol{\xi}_{n+1}^\top)$ ,  $\Gamma_m^+(0) = E(\boldsymbol{\xi}_{n+1}^+ \boldsymbol{\xi}_{n+1}^{+\top})$  and  $\Gamma_m^*(0) = E(\boldsymbol{\xi}_{n+1}^* \boldsymbol{\xi}_{n+1}^{*\top})$ . If Assumption 1 and 2 are satisfied, then,*

$$\|\Gamma_m^+(0) - \Gamma_m(0)\|_F = O_P\left(\frac{m^2}{\sqrt{p}}\right).$$

*If Assumption 1 and 2' are satisfied, then*

$$\|\Gamma_m^*(0) - \Gamma_m(0)\|_F = O_P\left(\frac{p^5 \sqrt{m}}{\lambda_m^2 \sqrt{n}} \sqrt{\sum_{j=1}^m \alpha_j^{-2}}\right).$$

**Proof:** Let  $\Psi_{j,p}$ ,  $\tilde{\Psi}_{j,p}$  and  $\hat{\Psi}_{j,p}$ ,  $j = 1, 2, \dots$ , be the coefficient matrices in the power series expansions of the inverse matrix polynomial  $(I_m - \sum_{j=1}^p A_{j,p} z^j)^{-1}$ ,  $(I_m - \sum_{j=1}^p \tilde{A}_{j,p} z^j)^{-1}$  and  $(I_m - \sum_{j=1}^p \hat{A}_{j,p} z^j)^{-1}$ , respectively, for  $|z| \leq 1$ , where  $I_m$  is the  $m \times m$  unit matrix. Set  $\Psi_{0,p} = \tilde{\Psi}_{0,p} = \hat{\Psi}_{0,p} = I_m$  and let  $\Sigma_e = E(\mathbf{e}_{t,p} \mathbf{e}_{t,p}^\top)$ ,  $\tilde{\Sigma}_e = E(\tilde{\mathbf{e}}_{t,p} \tilde{\mathbf{e}}_{t,p}^\top)$  and  $\hat{\Sigma}_e = E(\hat{\mathbf{e}}_{t,p} \hat{\mathbf{e}}_{t,p}^\top)$ . Since

$$\Gamma_m(0) = \sum_{j=0}^{\infty} \Psi_{j,p} \Sigma_e \Psi_{j,p}^\top, \quad \Gamma_m^+(0) = \sum_{j=0}^{\infty} \tilde{\Psi}_{j,p} \tilde{\Sigma}_e \tilde{\Psi}_{j,p}^\top \quad \text{and} \quad \Gamma_m^*(0) = \sum_{j=0}^{\infty} \hat{\Psi}_{j,p} \hat{\Sigma}_e \hat{\Psi}_{j,p}^\top,$$

the assertion of the lemma follows using the same arguments as in the proof of Lemma 6.5 of Paparoditis (2018) and the bounds

$$\sum_{j=1}^{\infty} \|\tilde{\Psi}_{j,p} - \Psi_{j,p}\|_F = O_P\left(m^{3/2}/\sqrt{p}\right) \quad \text{and} \quad \sum_{j=1}^{\infty} \|\hat{\Psi}_{j,p} - \tilde{\Psi}_{j,p}\|_F = O_P\left(\frac{p^5 \sqrt{m}}{\sqrt{n} \lambda_m^2} \sqrt{\sum_{j=1}^m \alpha_j^{-2}}\right),$$

obtained in the aforementioned paper. □

**Proof of Theorem 3.1:** Recall the notation  $\mathcal{X}_{n,k} = (\mathcal{X}_{n-k+1}, \mathcal{X}_{n-k+2}, \dots, \mathcal{X}_n)$ . Observe that

$$\|\widehat{g}(\mathcal{X}_{n,k}) - \widehat{g}^*(\mathcal{X}_{n,k})\|_2 \leq \|\widehat{g} - g_0\|_{\mathcal{L}} \|\mathcal{X}_{n,k}\|_2 + \|\widehat{g}^* - g_0\|_{\mathcal{L}} \|\mathcal{X}_{n,k}\|_2 = o_P(1)$$

where the last equality follows by Assumption 3 and the fact that  $\|\mathcal{X}_{n,k}\|_2 = O_P(1)$ , since  $\mathcal{X}_{n-k+1}, \mathcal{X}_{n-k+2}, \dots, \mathcal{X}_n$  are treated as fixed values. Thus

$$\mathcal{E}_{n+1} - \mathcal{E}_{n+1}^* = \sum_{j=1}^{\infty} \mathbf{1}_j^\top \boldsymbol{\xi}_{n+1} v_j - \left( \sum_{j=1}^m \mathbf{1}_j^\top \boldsymbol{\xi}_{n+1}^* \widehat{v}_j + U_{n+1,m}^* \right) + o_P(1)$$

and by Slutsky's theorem, it suffices to show that

$$d\left(\sum_{j=1}^{\infty} \mathbf{1}_j^\top \boldsymbol{\xi}_{n+1} v_j, \sum_{j=1}^m \mathbf{1}_j^\top \boldsymbol{\xi}_{n+1}^* \widehat{v}_j + U_{n+1,m}^*\right) = o_P(1). \quad (19)$$

Assertion (19) follows if we show that,

- (i)  $d\left(\sum_{j=1}^m \mathbf{1}_j^\top \boldsymbol{\xi}_{n+1}^+ v_j, \sum_{j=1}^{\infty} \mathbf{1}_j^\top \boldsymbol{\xi}_{n+1} v_j\right) \rightarrow 0$ ,
- (ii)  $\left\|\sum_{j=1}^m \mathbf{1}_j^\top \boldsymbol{\xi}_{n+1}^* \widehat{v}_j - \sum_{j=1}^m \mathbf{1}_j^\top \boldsymbol{\xi}_{n+1}^+ v_j\right\|_2 \xrightarrow{P} 0$ , and,
- (iii)  $U_{n+1,m}^* \xrightarrow{P} 0$ .

To establish (i) consider the sequence  $\{Y_n^+\}$  in  $\mathcal{H}$ , where  $Y_n^+ = \sum_{j=1}^{\infty} \widetilde{\xi}_{j,n+1} v_j$  and  $\widetilde{\xi}_{j,n+1} = \xi_{j,n+1}^+$  for  $j = 1, 2, \dots, m$  while  $\widetilde{\xi}_{j,n+1} = 0$  for  $j \geq m+1$ . For  $k \in \mathbb{N}$ , let  $Y_{n,k}^+ = \sum_{j=1}^k \widetilde{\xi}_{j,n+1} v_j$ . By Theorem 3.2 of Billingsley (1999), assertion (i) follows if we show that

- (a)  $Y_{n,k}^+ \xrightarrow{d} Y_k = \sum_{j=1}^k \xi_{j,n+1} v_j$  for any  $k \in \mathbb{N}$ , as  $n \rightarrow \infty$ .
- (b)  $Y_k \xrightarrow{d} Y = \sum_{j=1}^{\infty} \xi_{j,n+1} v_j$  as  $k \rightarrow \infty$ .
- (c) For any  $\epsilon > 0$ ,  $\lim_{k \rightarrow \infty} \limsup_{n \in \mathbb{N}} P(\|Y_{n,k}^+ - Y_n^+\|_2 > \epsilon) = 0$ .

Consider (a). Assume that  $n$  is large enough such that  $m > k$ . Since  $k$  is fixed,  $(\widetilde{\xi}_{1,n+1}, \widetilde{\xi}_{2,n+1}, \dots, \widetilde{\xi}_{k,n+1})^\top = (\xi_{1,n+1}^+, \xi_{2,n+1}^+, \dots, \xi_{k,n+1}^+)^\top = \boldsymbol{\xi}_{n+1}^+(k)$  where the latter vector is obtained as  $\boldsymbol{\xi}_{n+1}^+(k) = I_{m,k} \boldsymbol{\xi}_{n+1}$  with  $I_{m,k}$  the  $k \times m$  matrix having ones on the main diagonal and zero else, and the

vector  $\xi_{n+1}^+$  is generated via the regression type autoregression  $\xi_{n+1}^+ = \sum_{j=1}^p \tilde{A}_{j,p} \xi_{n+1-j} + e_{n+1}^+$ , which is driven by the i.i.d. innovations  $e_{n+1}^+$ . Therefore and since  $k$  is fixed, we have by standard arguments (see Lemma 3.1 of [Meyer and Kreiss \(2015\)](#)), that  $\xi_{n+1}^+(k) \xrightarrow{d} \xi_{n+1}(k) = (\xi_{1,n+1}, \xi_{2,n+1}, \dots, \xi_{k,n+1})^\top$ . By the continuous mapping theorem we then conclude that  $Y_{n,k}^+ \xrightarrow{d} \sum_{j=1}^k \xi_{j,n+1} v_j = Y_{n,k}$ . Consider (b). Notice that

$$E\|Y_k - Y\|_2^2 = E\left\|\sum_{j=k+1}^{\infty} \xi_{j,n+1} v_j\right\|_2^2 = \sum_{j=k+1}^{\infty} \lambda_j \rightarrow 0,$$

as  $k \rightarrow \infty$ , which by Markov's inequality and Slutsky's theorem implies that  $Y_k \xrightarrow{d} \sum_{j=1}^{\infty} \xi_{j,n+1} v_j$  as  $k \rightarrow \infty$ . Consider (c). Assume that  $m > k$ , otherwise  $Y_{n,k} - Y_n = 0$ . We have

$$\begin{aligned} E\|Y_{n,k} - Y_n\|_2^2 &= E\left\|\sum_{j=k+1}^m \xi_{j,n+1}^+ v_j\right\|_2^2 \\ &= \sum_{j=k+1}^m \mathbf{1}_j^\top \Gamma_m^+(0) \mathbf{1}_j \\ &= \sum_{j=k+1}^m \lambda_j + \sum_{j=k+1}^m \mathbf{1}_j^\top (\Gamma_m^+(0) - \Gamma_m(0)) \mathbf{1}_j. \end{aligned}$$

Now since

$$\left\|\sum_{j=k+1}^m \mathbf{1}_j^\top (\Gamma_m^+(0) - \Gamma_m(0)) \mathbf{1}_j\right\|_2 = O\left(\sqrt{m} \|\Gamma_m^+(0) - \Gamma_m(0)\|_F\right),$$

we get by Lemma A.1, Assumption 2 and Markov's inequality that

$$\limsup_{n \in \mathbb{N}} P(\|Y_{n,k}^+ - Y_n^+\|_2 > \epsilon) \leq \frac{1}{\epsilon^2} \sum_{j=k+1}^{\infty} \lambda_j,$$

which converges to zero as  $k \rightarrow \infty$ .

Consider assertion (ii). Since  $\|\widehat{v}_j\|_2 = 1$ , we get the bound

$$\begin{aligned}
\left\| \sum_{j=1}^m \mathbf{1}_j^\top (\boldsymbol{\xi}_{n+1}^+ v_j - \boldsymbol{\xi}_{n+1}^* \widehat{v}_j) \right\|_2 &\leq \left\| \sum_{j=1}^m \mathbf{1}_j^\top (\boldsymbol{\xi}_{n+1}^+ - \boldsymbol{\xi}_{n+1}^*) \widehat{v}_j \right\|_2 \\
&\quad + \left\| \sum_{j=1}^m \mathbf{1}_j^\top \boldsymbol{\xi}_{n+1}^+ (\widehat{v}_j - v_j) \right\|_2 \\
&\leq \sqrt{m} \|\boldsymbol{\xi}_{n+1}^* - \boldsymbol{\xi}_{n+1}^+\|_2 + \|\boldsymbol{\xi}_{n+1}^+\|_2 \sum_{j=1}^m \|\widehat{v}_j - v_j\|_2 \\
&= \sqrt{m} \|\boldsymbol{\xi}_{n+1}^* - \boldsymbol{\xi}_{n+1}^+\|_2 + O_P\left(\frac{m}{\sqrt{n}} \sqrt{\sum_{j=1}^m \alpha_j^{-2}}\right),
\end{aligned}$$

where the last equality follows using  $\|\boldsymbol{\xi}_{n+1}\|_2^2 = O_P(m)$  and Lemma 3.2 of Hörmann and Kokozska (2010). To evaluate the first term on the right hand side of the last displayed inequality, we use the bound

$$\begin{aligned}
\|\boldsymbol{\xi}_{n+1}^* - \boldsymbol{\xi}_{n+1}^+\|_2 &\leq \left\| \sum_{j=1}^p (\widehat{A}_{j,p} - \widetilde{A}_{j,p}) \widehat{\boldsymbol{\xi}}_{n+1-j} \right\|_2 + \left\| \sum_{j=1}^p \widetilde{A}_{j,p} (\widehat{\boldsymbol{\xi}}_{n+1-j} - \boldsymbol{\xi}_{n+1-j}) \right\|_2 \\
&\quad + \|\mathbf{e}_{n+1}^* - \mathbf{e}_{n+1}^+\|_2 \\
&= \sum_{j=1}^3 T_{j,n},
\end{aligned} \tag{20}$$

with an obvious notation for  $T_{j,n}$ ,  $j = 1, 2, 3$ . We have using  $\|\widehat{A}_p - \widetilde{A}_p\|_F = O_P((p\sqrt{m}\lambda_m^{-1} + p^2)^2 \sqrt{n^{-1} \sum_{j=1}^m \alpha_j^{-2}})$ , see Paparoditis (2018), p. 5 of the Supplementary Material, that

$$\begin{aligned}
T_{1,n} &= \left\| \sum_{j=1}^p (\widehat{A}_{j,p} - \widetilde{A}_{j,p}) \widehat{\boldsymbol{\xi}}_{n+1-j} \right\|_2 \leq \sum_{j=1}^p \|\widehat{A}_{j,p} - \widetilde{A}_{j,p}\|_F \|\widehat{\boldsymbol{\xi}}_{n+1-j}\|_2 \\
&= O_P\left(\sqrt{m} \sum_{j=1}^p \|\widehat{A}_{j,p} - \widetilde{A}_{j,p}\|_F\right) \\
&= O_P(\sqrt{mp} \|\widehat{A}_p - \widetilde{A}_p\|_F) \\
&= O_P\left(\frac{m^{3/2} p^{5/2}}{\lambda_m^2} \sqrt{\frac{1}{n} \sum_{j=1}^m \alpha_j^{-2}}\right) \rightarrow 0,
\end{aligned}$$

by Assumption 2. Furthermore, by the same assumption,

$$\begin{aligned}
T_{2,n}^2 &= \left\| \sum_{j=1}^p \tilde{A}_{j,p} (\hat{\xi}_{n+1-j} - \xi_{n+1-j}) \right\|_2^2 \leq \sum_{j=1}^p \|\tilde{A}_{j,p}\|_F^2 \sum_{j=1}^p \|\hat{\xi}_{n+1-j} - \xi_{n+1-j}\|_2^2 \\
&\leq \sum_{j=1}^p \|\tilde{A}_{j,p}\|_F^2 \sum_{i=1}^p \|\mathcal{X}_{n+1-i}\|_2^2 \sum_{l=1}^m \|\hat{v}_l - v_l\|_2^2 \\
&= O_P\left(p \sum_{l=1}^m \|\hat{v}_l - v_l\|_2^2\right) \\
&= O_P\left(pn^{-1} \sum_{l=1}^m \alpha_l^{-2}\right) \rightarrow 0.
\end{aligned}$$

Finally, for the the last term on the right hand side of (20),  $E\|e_{n+1}^* - e_{n+1}^+\|_2^2 \rightarrow 0$  in probability, follows as in the proof of Lemma 6.7 in Paparoditis (2018).

Assertion (iii) follows from Markov's inequality and the fact that  $E^*\|U_{n+1,m}^*\|_2^2 \rightarrow 0$  in probability. The last statement is true since

$$\begin{aligned}
E^*\|U_{n+1,m}^*\|_2^2 &= \frac{1}{n} \sum_{t=1}^n \|\hat{U}_{t,m} - \bar{U}_n\|_2^2 \\
&\leq \frac{4}{n} \sum_{t=1}^n \|\hat{U}_{t,m} - U_{t,m}\|_2^2 + \frac{4}{n} \sum_{t=1}^n \|U_{t,m}\|_2^2 + 2\|\bar{U}_n\|_2^2 \\
&= \frac{4}{n} \sum_{t=1}^n \left\| \sum_{j=1}^m \mathbf{1}_j^\top (\xi_t v_j - \hat{\xi}_t \hat{v}_j) \right\|_2^2 + o_P(1)
\end{aligned}$$

where the  $o_P(1)$  is due to the weak law of large numbers and the fact that  $E\|U_{t,m}\|^2 = \sum_{j=m+1}^\infty \lambda_j \rightarrow 0$  as  $m \rightarrow \infty$  and  $\bar{U}_{n,m} \rightarrow 0$ , in probability. Furthermore, for the first term on the right hand side of the last displayed equality we have the bound

$$\begin{aligned}
&\leq \frac{8}{n} \sum_{t=1}^n \left\| \sum_{j=1}^m \mathbf{1}_j^\top (\hat{\xi}_t - \xi_t) \hat{v}_j \right\|_2^2 + \frac{8}{n} \sum_{t=1}^n \left\| \sum_{j=1}^m \mathbf{1}_j^\top \xi_t (\hat{v}_j - v_j) \right\|_2^2 \\
&\leq \frac{8}{n} \sum_{t=1}^n \|\mathcal{X}_t\|_2^2 \sum_{j=1}^m \|\hat{v}_j - v_j\|_2^2 + 8 \sqrt{\sum_{j,l=1}^m \left| \frac{1}{n} \sum_{t=1}^n \xi_{j,t} \xi_{l,t} \right|_2^2} \sum_{j=1}^m \|\hat{v}_j - v_j\|_2^2 \\
&= O_P\left(n^{-1} \sum_{j=1}^m \alpha_j^{-2}\right) \rightarrow 0,
\end{aligned}$$

where the last equality follows because  $n^{-1} \sum_{t=1}^n \|\mathcal{X}_t\|_2^2 = O_P(1)$  and  $n^{-1} \sum_{t=1}^n \xi_{j,t} \xi_{l,t} \xrightarrow{P} \lambda_j \mathbf{1}_{j=l}$

as  $n \rightarrow \infty$ . □

**Proof of Theorem 3.2:** We only give the proof of assertion (17) since the weak convergence of the conditional distribution of  $\mathcal{E}_{n+1}^* | \mathcal{X}_{n,k}$  to the corresponding conditional distribution of  $\mathcal{E}_{n+1} | \mathcal{X}_{n,k}$ , has been given under weaker assumptions in the proof of Theorem 3.1. We have

$$\begin{aligned} |\sigma_{n+1}^{*2}(\tau) - \sigma_{n+1}^2(\tau)| &\leq |E^*(\mathcal{X}_{n+1}^*(\tau)^2 - E(\mathcal{X}_{n+1}(\tau))^2| \\ &\quad + 2|E^*X_{n+1}^*(\tau)(\widehat{g}^*(\mathcal{X}_{n,k})(\tau) - g_0(\mathcal{X}_{n,k})(\tau))| + 2|EX_{n+1}(\tau)(\widehat{g}(\mathcal{X}_{n,k})(\tau) - g_0(\mathcal{X}_{n,k})(\tau))| \\ &\quad + |E^*(\widehat{g}^*(\mathcal{X}_{n,k})(\tau))^2 - g_0^2(\mathcal{X}_{n,k})(\tau)| + |E(\widehat{g}(\mathcal{X}_{n,k})(\tau))^2 - g_0^2(\mathcal{X}_{n,k})(\tau)| \end{aligned} \quad (21)$$

Since  $\sup_{\tau \in [0,1]} E^*(X_{n+1}^*(\tau))^2 = \sup_{\tau \in [0,1]} \widehat{c}(\tau, \tau) = O_P(1)$  and  $\sup_{\tau \in [0,1]} E(X_{n+1}(\tau))^2 = \sup_{\tau \in [0,1]} c(\tau, \tau) < \infty$ , by the continuity of the kernel  $c$ , we get using Cauchy-Schwarz's inequality and Assumption 3' that

$$\begin{aligned} \sup_{\tau \in [0,1]} |E^*X_{n+1}^*(\tau)(\widehat{g}^*(\mathcal{X}_{n,k})(\tau) - g_0(\mathcal{X}_{n,k})(\tau))| \\ \leq \sup_{\tau \in [0,1]} E^*(X_{n+1}^*(\tau))^2 \sqrt{\sup_{\tau \in [0,1]} E^*(\widehat{g}^*(\mathcal{X}_{n,k})(\tau) - g_0(\mathcal{X}_{n,k})(\tau))^2} \rightarrow 0, \end{aligned}$$

and

$$\begin{aligned} \sup_{\tau \in [0,1]} |EX_{n+1}(\tau)(\widehat{g}(\mathcal{X}_{n,k})(\tau) - g_0(\mathcal{X}_{n,k})(\tau))| \\ \leq \sup_{\tau \in [0,1]} E(X_{n+1}(\tau))^2 \sqrt{\sup_{\tau \in [0,1]} E(\widehat{g}(\mathcal{X}_{n,k})(\tau) - g_0(\mathcal{X}_{n,k})(\tau))^2} \rightarrow 0, \end{aligned}$$

Using  $a^2 - b^2 = (a - b)(a + b)$ , Cauchy-Schwarz's inequality and Assumption 3' again, we get for the last two term on the right hand side of the bound (21), that they also converges uniformly to zero, in probability. It remain to show that

$$\sup_{\tau \in [0,1]} |E^*(\mathcal{X}_{n+1}^*(\tau)^2 - E(\mathcal{X}_{n+1}(\tau))^2| \rightarrow 0, \quad (22)$$

in probability. Notice first that due to the independence of  $\sum_{j=1}^m \mathbf{1}^\top \boldsymbol{\xi}_{n+1}^* \widehat{v}_j$  and  $U_{n+1,m}^*$  we have that  $E^*(\mathcal{X}_{n+1}^*(\tau))^2 = E^*(\sum_{j=1}^m \mathbf{1}^\top \boldsymbol{\xi}_{n+1}^* \widehat{v}_j(\tau))^2 + E^*(U_{n+1,m}^*(\tau))^2$ . Furthermore, using  $c(\tau, \tau) =$

$\sum_{j=1}^{\infty} \lambda_j v_j^2(\tau)$ , where the convergence is uniformly in  $\tau \in [0, 1]$ , we get that

$$\sup_{\tau \in [0, 1]} E(U_{n+1, m}(\tau))^2 = \sup_{\tau \in [0, 1]} \sum_{j=m+1}^{\infty} \lambda_j v_j^2(\tau) \rightarrow 0.$$

Therefore, and because  $E(X_{n+1, m}(\tau)U_{n+1, m}(\tau)) = 0$  for all  $\tau \in [0, 1]$ , to establish (22), it suffices by Cauchy-Schwarz inequality and the inequality  $\sup_{\tau \in [0, 1]} \sqrt{f(\tau)} \leq \sqrt{\sup_{\tau \in [0, 1]} f(\tau)}$ , where  $f$  is a non negative function on  $[0, 1]$ , to show that

- (a)  $\sup_{\tau \in [0, 1]} |E(\sum_{j=1}^m \mathbf{1}_j^\top (\boldsymbol{\xi}_{n+1}^* \widehat{v}_j(\tau))^2 - E(\sum_{j=1}^m \mathbf{1}_j^\top \boldsymbol{\xi}_{n+1} v_j(\tau))^2| \rightarrow 0$ , and
- (b)  $\sup_{\tau \in [0, 1]} E^*(U_{n+1, m}^*(\tau))^2 \rightarrow 0$ ,

in probability.

Consider (a). We have

$$\begin{aligned} |E(\sum_{j=1}^m \mathbf{1}_j^\top (\boldsymbol{\xi}_{n+1}^* \widehat{v}_j(\tau))^2 - E(\sum_{j=1}^m \mathbf{1}_j^\top \boldsymbol{\xi}_{n+1} v_j(\tau))^2| &\leq | \sum_{j_1, j_2=1}^m \mathbf{1}_{j_1}^\top (\Gamma_m^*(0) - \Gamma_m(0)) \mathbf{1}_{j_2} v_{j_1}(\tau) v_{j_2}(\tau) | \\ &\quad + | \sum_{j_1, j_2=1}^m \mathbf{1}_{j_1}^\top \Gamma_m^*(0) \mathbf{1}_{j_2} (\widehat{v}_{j_1}(\tau) \widehat{v}_{j_2}(\tau) - v_{j_1}(\tau) v_{j_2}(\tau)) | \\ &\leq \|\Gamma_m^*(0) - \Gamma_m(0)\|_F (\sum_{j=1}^m |v_j(\tau)|) \\ &\quad + \|\Gamma_m(0)\|_F \sum_{j=1}^m |\widehat{v}_j(\tau) - v_j(\tau)| (\sum_{j=1}^m |v_j(\tau)| + \sum_{j=1}^m |\widehat{v}_j(\tau)|). \end{aligned}$$

To evaluate the above terms notice that  $\|\Gamma_m(0)\|_F = O(1)$  and because of Lemma A.1,  $\|\Gamma_m^*(0)\|_F = O_P(1)$ , where both  $O_P(1)$  bounds are uniform in  $m$ . Furthermore, using  $c(\tau, \tau) = \sum_{j=1}^{\infty} \lambda_j v_j^2(\tau)$  we get by the continuity of the kernel  $c(\cdot, \cdot)$  on the compact support  $[0, 1] \times [0, 1]$ , the bound

$$\sum_{j=1}^m \lambda_j v_j^2(\tau) \leq c(\tau, \tau) \Rightarrow \sup_{\tau \in [0, 1]} \sum_{j=1}^m v_j^2(\tau) \leq \frac{1}{\lambda_m} C,$$

where  $C := \sup_{\tau \in [0, 1]} c(\tau, \tau) < \infty$ . Moreover, arguing as in Kokoszka and Reimherr (2013a), which showed that  $(\sqrt{n}(\widehat{v}_j - v_j), j = 1, 2, \dots, m)$  converges weakly on  $\mathcal{H} \times \mathcal{H} \times \dots \times \mathcal{H}$ , we get that  $\{m^{-1} \sum_{j=1}^m (\sqrt{n}(\widehat{v}_j(\tau) - v_j(\tau)))^2, \tau \in [0, 1]\}$  converges weakly on  $\mathcal{H}$ , which by the con-



tinuous mapping theorem implies that  $\sup_{\tau \in [0,1]} m^{-1} \sum_{j=1}^m n(\widehat{v}_j(\tau) - v_j(\tau))^2 = O_P(1)$ . Hence

$$\sum_{j=1}^m |\widehat{v}_j(\tau)| \leq \sqrt{m} \sqrt{\sum_{j=1}^m v_j^2(\tau)} + \sqrt{m} \sqrt{\sum_{j=1}^m (\widehat{v}_j(\tau) - v_j(\tau))^2} = O\left(\sqrt{\frac{m}{\lambda_m}} + \frac{m}{\sqrt{n}}\right),$$

and

$$\sum_{j=1}^m |\widehat{v}_j(\tau) - v_j(\tau)| \left( \sum_{j=1}^m |v_j(\tau)| + \sum_{j=1}^m |\widehat{v}_j(\tau)| \right) = O_P\left(\frac{m^{3/2}}{n\lambda_m^{1/2}} + \frac{m^2}{n^{3/2}}\right).$$

We therefore have,

$$\sup_{\tau \in [0,1]} \left| E\left(\sum_{j=1}^m \mathbf{1}_j^\top (\boldsymbol{\xi}_{n+1}^* \widehat{v}_j(\tau))\right)^2 - E\left(\sum_{j=1}^m \mathbf{1}_j^\top \boldsymbol{\xi}_{n+1} v_j(\tau)\right)^2 \right| = O_P\left(\sqrt{\frac{m}{\lambda_m}} \|\Gamma_m^*(0) - \Gamma_m(0)\|_F\right) + o_P(1),$$

which vanishes because of Lemma A.1 and Assumption 2'.

Consider (b). Since  $E^*(U_{n+1,m}^*(\tau))^2 \leq 2n^{-1} \sum_{t=1}^n (\widehat{U}_{t,n}^2(\tau))^2 + 2(\overline{U}_n(\tau))^2$ , it suffices to show that  $\sup_{\tau \in [0,1]} n^{-1} \sum_{t=1}^n (\widehat{U}_{t,n}(\tau))^2 \rightarrow 0$ . Toward this we use the bound

$$\begin{aligned} \frac{1}{n} \sum_{t=1}^n (\widehat{U}_{t,n}(\tau))^2 &\leq \frac{4}{n} \sum_{t=1}^n \|\widehat{\boldsymbol{\xi}}_t - \boldsymbol{\xi}_t\|_2^2 \sum_{j=1}^m v_j^2(\tau) + \frac{4}{n} \sum_{t=1}^n \|\widehat{\boldsymbol{\xi}}_{n+1}\|_2^2 \sum_{j=1}^m (\widehat{v}_j(\tau) - v_j(\tau))^2 \\ &\quad + \frac{2}{n} \sum_{t=1}^n \left( \sum_{j=m+1}^{\infty} \zeta_{j,t} v_j(\tau) \right)^2. \end{aligned} \tag{23}$$

Since

$$\sup_{\tau \in [0,1]} \frac{1}{n} \sum_{t=1}^n \|\widehat{\boldsymbol{\xi}}_t - \boldsymbol{\xi}_t\|_2^2 \sum_{j=1}^m v_j^2(\tau) \leq C \frac{1}{\lambda_m} \frac{1}{n} \sum_{t=1}^n \|\widehat{\boldsymbol{\xi}}_t - \boldsymbol{\xi}_t\|_2^2 = \frac{1}{\lambda_m} O_P\left(\frac{1}{n} \sum_{j=1}^m \frac{1}{\alpha_j^2}\right)$$

and

$$\sup_{\tau \in [0,1]} \frac{1}{n} \sum_{t=1}^n \|\widehat{\boldsymbol{\xi}}_{n+1}\|_2^2 \sum_{j=1}^m (\widehat{v}_j(\tau) - v_j(\tau))^2 \leq O_P\left(\frac{m}{n}\right) \frac{1}{n} \sum_{t=1}^n \|\widehat{\boldsymbol{\xi}}_t\|_2^2 = O_P\left(\frac{m}{n}\right),$$

the first two terms on the right hand side of (23) converge to zero. For the third term we get

after evaluating the squared term and substituting  $\xi_{j,t} = \langle \mathcal{X}_t, v_j \rangle$  the bound

$$\begin{aligned} \frac{1}{n} \sum_{t=1}^n (\mathcal{X}_t(\tau) - \sum_{j=1}^m \xi_{j,t} v_j(\tau))^2 &\leq \left| \frac{1}{n} \sum_{t=1}^n \mathcal{X}_t^2(\tau) - E \mathcal{X}_t^2(\tau) \right| \\ &\quad + \left| \sum_{j_1=1}^m \sum_{j_2=1}^m \langle (\hat{\mathcal{C}}_0 - \mathcal{C}_0)(v_{j_1}), v_{j_2} \rangle v_{j_1}(\tau) v_{j_2}(\tau) \right| \\ &\quad + 2 \left| \sum_{j=1}^m \int_0^1 (\hat{c}(\tau, s) - c(\tau, s)) v_j(s) ds v_j(\tau) \right| + \left| E \mathcal{X}_t^2(\tau) - \sum_{j=1}^m \lambda_j v_j^2(\tau) \right|. \end{aligned} \quad (24)$$

Now,  $\sup_{\tau \in [0,1]} |n^{-1} \sum_{t=1}^n (\mathcal{X}_t^2(\tau) - E \mathcal{X}_t^2(\tau))| = O_P(n^{-1/2}) \rightarrow 0$  by the continuous mapping theorem and since  $\{n^{-1/2} \sum_{t=1}^n (\mathcal{X}_t^2(\tau) - E \mathcal{X}_t^2(\tau)), \tau \in [0, 1]\}$  converges weakly on  $\mathcal{H}$ . Furthermore,  $\sup_{\tau \in [0,1]} |E \mathcal{X}_t^2(\tau) - \sum_{j=1}^m \lambda_j v_j^2(\tau)| \rightarrow 0$  by Theorem 7.3.5 of [Hsing and Eubank \(2015\)](#). Also

$$\begin{aligned} \sup_{\tau \in [0,1]} \left| \sum_{j_1=1}^m \sum_{j_2=1}^m \langle (\hat{\mathcal{C}}_0 - \mathcal{C}_0)(v_{j_1}), v_{j_2} \rangle v_{j_1}(\tau) v_{j_2}(\tau) \right| &\leq \|\hat{\mathcal{C}}_0 - \mathcal{C}_0\|_{HS} \sup_{\tau \in [0,1]} \left( \sum_{j=1}^m |v_j(\tau)| \right)^2 \\ &\leq m \|\hat{\mathcal{C}}_0 - \mathcal{C}_0\|_{HS} \sup_{\tau \in [0,1]} \sum_{j=1}^m v_j^2(\tau) \\ &\leq C \frac{m}{\lambda_m} \|\hat{\mathcal{C}}_0 - \mathcal{C}_0\|_{HS} = O_P\left(\frac{m}{\sqrt{n} \lambda_m}\right), \end{aligned}$$

which converges to zero. Finally,

$$\begin{aligned} \left| \sum_{j=1}^m \int_0^1 (\hat{c}(\tau, s) - c(\tau, s)) v_j(s) ds v_j(\tau) \right|^2 &\leq \int_0^1 (\hat{c}(\tau, s) - c(\tau, s))^2 ds \left( \sum_{j=1}^m |v_j(\tau)| \right)^2 \\ &\leq \int_0^1 (\hat{c}(\tau, s) - c(\tau, s))^2 ds m \sum_{j=1}^m v_j^2(\tau), \end{aligned}$$

and therefore,

$$\begin{aligned} \sup_{\tau \in [0,1]} \left| \sum_{j=1}^m \int_0^1 (\hat{c}(\tau, s) - c(\tau, s)) v_j(s) ds v_j(\tau) \right| &\leq C \sqrt{\frac{m}{\lambda_m}} \sqrt{\sup_{\tau \in [0,1]} \int_0^1 (\hat{c}(\tau, s) - c(\tau, s))^2 ds} \\ &= O_P\left(\sqrt{\frac{m}{\lambda_m n}}\right), \end{aligned}$$

which converges to zero. □

## References

- Antoniadis, A., Paparoditis, E. and Sapatinas, T. (2006), 'A functional wavelet-kernel approach for time series prediction', *Journal of the Royal Statistical Society: Series B* **68**(5), 837–857.
- Aue, A., Norinho, D. D. and Hörmann, S. (2015), 'On the prediction of stationary functional time series', *Journal of the American Statistical Association: Theory and Methods* **110**(509), 378–392.
- Berlinet, A., Elamine, A. and Mas, A. (2011), 'Local linear regression for functional data', *Annals of the Institute of Statistical Mathematics* **63**(5), 1047–1075.
- Billingsley, P. (1999), *Converges of Probability Measures*, John Wiley & Sons, New York.
- Boj, E., Delicado, P. and Fortiana, J. (2010), 'Distance-based local linear regression for functional predictors', *Computational Statistics & Data Analysis* **54**(2), 429–437.
- Bosq, D. (2000), *Linear processes in function spaces*, Lecture notes in Statistics, New York.
- Bosq, D. and Blanke, D. (2007), *Inference and Prediction in Large Dimensions*, John Wiley & Sons, Chichester.
- Breidt, F. J., Davis, R. A. and Dunsmuir, W. T. M. (1995), 'Improved bootstrap prediction intervals for autoregressions', *Journal of Time Series Analysis* **16**(2), 177–200.
- Cheng, R. and Pourahmadi, M. (1993), 'Baxter's inequality and convergence of finite predictors of multivariate stochastic processes', *Probability Theory and Related Fields* **95**, 115–124.
- Chiou, J.-M. and Müller, H.-G. (2009), 'Modeling hazard rates as functional data for the analysis of cohort lifetables and mortality forecasting', *Journal of the American Statistical Association: Applications and Case Studies* **104**(486), 572–585.
- Cuevas, A., Febrero, M. and Fraiman, R. (2006), 'On the use of the bootstrap for estimating functions with functional data', *Computational Statistics and Data Analysis* **51**(2), 1063–1074.
- Dehling, H., Sharipov, S. O. and Wendler, M. (2015), 'Bootstrap for dependent Hilbert space-valued random variables with application to von Mises statistics', *Journal of Multivariate Analysis* **133**, 200–215.

- Ferraty, F. and Vieu, P. (2006), *Nonparametric Functional Data Analysis*, Springer, New York.
- Ferraty, F. and Vieu, P. (2011), Kernel regression estimation for functional data, *in* F. Ferraty and Y. Romain, eds, 'The Oxford Handbook of Functional Data Analysis', Oxford University Press, Oxford.
- Findley, D. F. (1986), Bootstrap estimates of forecast mean square errors for autoregressive processes, *in* D. M. Allen, ed., 'Computer Science and Statistics: the Interface', Elsevier Science, pp. 11–17.
- Franke, J. and Nyarige, E. G. (2019), A residual-based bootstrap for functional autoregressions, Technical report, University of Kaiserslautern.  
URL: <https://arxiv.org/abs/1905.07635>
- Gneiting, T. and Raftery, A. E. (2007), 'Strictly proper scoring rules, prediction and estimation', *Journal of the American Statistical Association: Review Article* **102**(477), 359–378.
- Goldsmith, J., Greven, S. and Crainiceanu, C. (2013), 'Corrected confidence bands for functional data using principal components', *Biometrics* **69**(1), 41–51.
- Hörmann, S., Kidziński, L. and Hallin, M. (2015), 'Dynamic functional principal components', *Journal of the Royal Statistical Society: Series B* **77**(2), 319–348.
- Hörmann, S. and Kokoszka, P. (2010), 'Weakly dependent functional data', *Annals of Statistics* **38**(3), 1845–1884.
- Hörmann, S. and Kokoszka, P. (2012), Functional time series, *in* T. S. Rao, S. S. Rao and C. R. Rao, eds, 'Handbook of Statistics', Vol. 30, North Holland, Amsterdam, pp. 157–186.
- Horváth, L. and Kokoszka, P. (2012), *Inference for Functional Data with Applications*, Springer, New York.
- Horváth, L., Kokoszka, P. and Rice, G. (2014), 'Testing stationarity of functional time series', *Journal of Econometrics* **179**(1), 66–82.
- Hsing, T. and Eubank, R. (2015), *Theoretical Foundations of Functional Data Analysis, with An Introduction to Linear Operators*, John Wiley & Sons, New York.

- Hurvich, C. M. and Tsai, C.-L. (1993), 'A corrected Akaike information criterion for vector autoregressive model selection', *Journal of Time Series Analysis* **14**(3), 271–279.
- Hyndman, R. J. and Shang, H. L. (2009), 'Forecasting functional time series (with discussions)', *Journal of the Korean Statistical Society* **38**(3), 199–221.
- Kokoszka, P. and Reimherr, M. (2013a), 'Asymptotic normality of the principal components of functional time series', *Stochastic Processes and Their Applications* **123**(5), 1546–1562.
- Kokoszka, P. and Reimherr, M. (2013b), 'Determining the order of the functional autoregressive model', *Journal of Time Series Analysis* **34**(1), 116–129.
- Kokoszka, P., Rice, G. and Shang, H. L. (2017), 'Inference for the autocovariance of a functional time series under conditional heteroscedasticity', *Journal of Multivariate Analysis* **162**, 32–50.
- Kudraszow, N. L. and Vieu, P. (2013), 'Uniform consistency of  $k$ NN regressors for functional variables', *Statistics and Probability Letters* **83**(8), 1863–1870.
- Masry, E. (2005), 'Nonparametric regression estimation for dependent functional data: asymptotic normality', *Stochastic Processes and their Applications* **115**(1), 155–177.
- McMurry, T. and Politis, D. N. (2011), Resampling methods for functional data, in F. Ferraty and Y. Romain, eds, 'The Oxford Handbook of Functional Data Analysis', Oxford University Press, New York, pp. 189–209.
- Meyer, M. and Kreiss, J.-P. (2015), 'On the vector autoregressive sieve bootstrap', *Journal of Time Series Analysis* **36**(3), 377–397.
- Pan, L. and Politis, D. N. (2016), 'Bootstrap prediction intervals for linear, nonlinear and nonparametric autoregression', *Journal of Statistical Planning and Inference* **177**, 1–27.
- Panaretos, V. M. and Tavakoli, S. (2013), 'Fourier analysis of stationary time series in function space', *The Annals of Statistics* **41**(2), 568–603.
- Paparoditis, E. (2018), 'Sieve bootstrap for functional time series', *Annals of Statistics* **46**(6B), 3510–3538.

- Paparoditis, E. and Sapatinas, T. (2016), 'Bootstrap-based testing of equality of mean functions or equality of covariance operators for functional data', *Biometrika* **103**(3), 727–733.
- Pilavakis, D., Paparoditis, E. and Sapatinas, T. (2019), 'Moving block and tapered block bootstrap for functional time series with an application to the  $K$ -sample mean problem', *Bernoulli* **25**(4B), 3496–3526.
- Politis, D. N. and Romano, J. (1994a), 'Limit theorems for weakly dependent Hilbert space valued random variables with applications to the stationary bootstrap', *Statistica Sinica* **4**(2), 461–476.
- Politis, D. N. and Romano, J. P. (1994b), 'The stationary bootstrap', *Journal of the American Statistical Association: Theory and Methods* **89**(428), 1303–1313.
- Raña, P., Aneiros-Perez, G. and Vilar, J. M. (2015), 'Detection of outliers in functional time series', *Environmetrics* **26**(3), 178–191.
- Shang, H. L. (2015), 'Resampling techniques for estimating the distribution of descriptive statistics of functional data', *Communications in Statistics-Simulation and Computation* **44**(3), 614–635.
- Shang, H. L. (2017), 'Functional time series forecasting with dynamic updating: An application to intraday particulate matter concentration', *Econometrics and Statistics* **1**, 184–200.
- Shang, H. L. (2018), 'Bootstrap methods for stationary functional time series', *Statistics and Computing* **28**(1), 1–10.